Available online at www.sciencedirect.com
SCIENCE DIRECT®
Tectonophysics 367 (2003) 253–278
TECTONOPHYSICS
www.elsevier.com/locate/tecto

Early formed regional antiforms and synforms that fold younger matrix schistosities: their effect on sites of mineral growth

T.H. Bell*, A.P. Ham, K.A. Hickey

School of Earth Sciences, James Cook University, Townsville, Queensland 4811, Australia

Received 28 January 2002; accepted 19 March 2003

Abstract

In the metamorphic cores of many orogenic belts, large macroscopic folds in compositional layering also appear to fold one or more pervasive matrix foliations. The latter geometry suggests the folds formed relatively late in the tectonic history, after foliation development. However, microstructural analysis of four examples of such folds suggests this is not the case. The folds formed relatively early in the orogenic history and are the end product of multiple, near orthogonal, overprinting bulk shortening events. Once large macroscopic folds initiate, they may tighten further during successive periods of sub-parallel shortening, folding or reactivation of foliations that develop during intervening periods of near orthogonal shortening. Reactivation of the compositional layering defining the fold limbs causes foliation to be rotated into parallelism with the limbs.

Multiple periods of porphyroblast growth accompanied the multiple phases of deformation that postdated the initial development of these folds. Some of these phases of deformation were attended by the development of large numbers of same asymmetry spiral-shaped inclusion trails in porphyroblasts on one limb of the fold and not the other, or larger numbers of opposite asymmetry spirals on the other limb, or similar numbers of the same asymmetry spirals on both limbs. Significantly, the largest disparity in numbers from limb to limb occurred for the first of these cases. For all four regional folds examined, the structural relationships that accompanied these large disparities were identical. In each case the shear sense operating on steeply dipping foliations was opposite to that required to originally develop the fold. Reactivation of the folded compositional layering was not possible for this shear sense. This favoured the development of sites of approximately coaxial shortening early during the deformation history, enhancing microfracture and promoting the growth of porphyroblasts on this limb in comparision to the other. These distributions of inclusion trail geometries from limb to limb cannot be explained by porphyroblast rotation, or folding of pre-existing rotated porphyroblasts within a shear zone, but can be explained by development of the inclusion trails synchronous with successive sub-vertical and sub-horizontal foliations.

Keywords: Cleavage asymmetry; Overprinting asymmetries; Crenulation cleavage; Fold mechanisms; Inclusion trail asymmetry; Porphyroblast nucleation and growth

1. Introduction

Regional scale folds in compositional layering are one of the most spectacular products of orogenesis in crustal rocks. Determining the timing of initial devel-

* Corresponding author.
E-mail address: tim.bell@jcu.edu.au (T.H. Bell).

0040-1951/03/$ - see front matter © 2003 Elsevier Science B.V. All rights reserved.
doi:10.1016/S0040-1951(03)00126-4

opment of these regional folds, relative to the formation of various matrix cleavages, is difficult because of their size. For example, determining whether a mesoscopic foliation on a regional fold limb is one that has

1. been folded,
2. formed as an axial plane fabric when the fold developed,
3. formed sub-parallel to the axial plane in a subsequent event,

can be quite problematic and an incorrect determination can impinge considerably on the genesis interpreted for that fold. A major ingredient in understanding the origin of regional folds is the determination of their timing relative to the history of deformation preserved at the microscopic and mesoscopic scales. Deciding the timing of a fold relative to a deformation sequence has historically been treated as a simple matter based around whether a foliation lies parallel to the axial plane or appears to be folded by the fold. However, timing folds in this manner is not simple. For example, in the Adelaide fold belt, folds that appear to bend a cleavage have been demonstrated to have initially formed earlier than both the cleavage that has been folded and the cleavage that is now axial planar to the fold (Adshead-Bell and Bell, 1999). In some multiply and complexly deformed terrains, none of the foliations preserved in porphyroblasts or the matrix show any definite genetic relationship to mapped folds (Hickey and Bell, 2001). Apparently simple macroscopic folds that fold a foliation can be composite structures that formed earlier than the fabric they deform, their present geometry being a consequence of a long complex history of overprinting deformations. We believe such folds are relatively ubiquitous and that most large macroscopic folds that deform a foliation need to be re-examined. Determining the spatial and temporal evolution of such folds has important implications for understanding patterns and processes of orogenic deformation.

In this study, we present evidence for a long-lived and complex deformation history associated with the development of four large macroscopic fold structures. This interpretation emanated from earlier studies that attempted to test whether early-formed porphyroblasts have been rotated from limb to limb around younger macroscopic folds. Analysis of matrix and porphyroblast microstructures revealed that all but one of the regional fold structures initiated prior to development of the foliations that are folded around them (e.g., Adshead-Bell and Bell, 1999; Hickey and Bell, 2001). Patterns of inclusion trail asymmetry preserved in porphyroblasts around the four folds provide criteria on the timing of folding. They also reveal evidence for the previously unrecognized influence of a pre-existing fold geometry on the pattern of porphyroblast nucleation and growth. Of particular importance is the role of reactivation, or shearing, of compositional layering in determining sites of porphyroblast nucleation.

2. Timing folds relative to foliations

An important aspect of timing fold development is determining the extent to which shortening has been accommodated by the reactivation, rather than the crenulation of a folded foliation. Equally important is determining the asymmetry of folded foliations relative to differentiated crenulation cleavages that develop parallel to the axial plane of the fold. There are two quite different types of cleavage asymmetry and they commonly have contrasting geometries across a fold hinge. Distinguishing the difference between these asymmetry types has considerable significance for understanding the timing and kinematic development of a fold. We call them ‘‘vergence’’ asymmetry and ‘‘differentiation’’ asymmetry and note that only the former has been clearly described in textbooks. A review of foliation reactivation and cleavage asymmetry in the matrix and within porphyroblasts is presented below.

2.1. Reactivation of folded foliations

Reactivation of an older foliation ($S_{0,1}$ in Fig. 1a) on the limb of a fold is conceived as occurring when synthetic shear operating on a newly developing foliation (anticlockwise shear on S_2 in Fig. 1a) switches to antithetic shear on the older foliation. The principal of the process is shown in Fig. 1b using a card deck. Here, anticlockwise shear on the boundary of the cards is accommodated by clock-

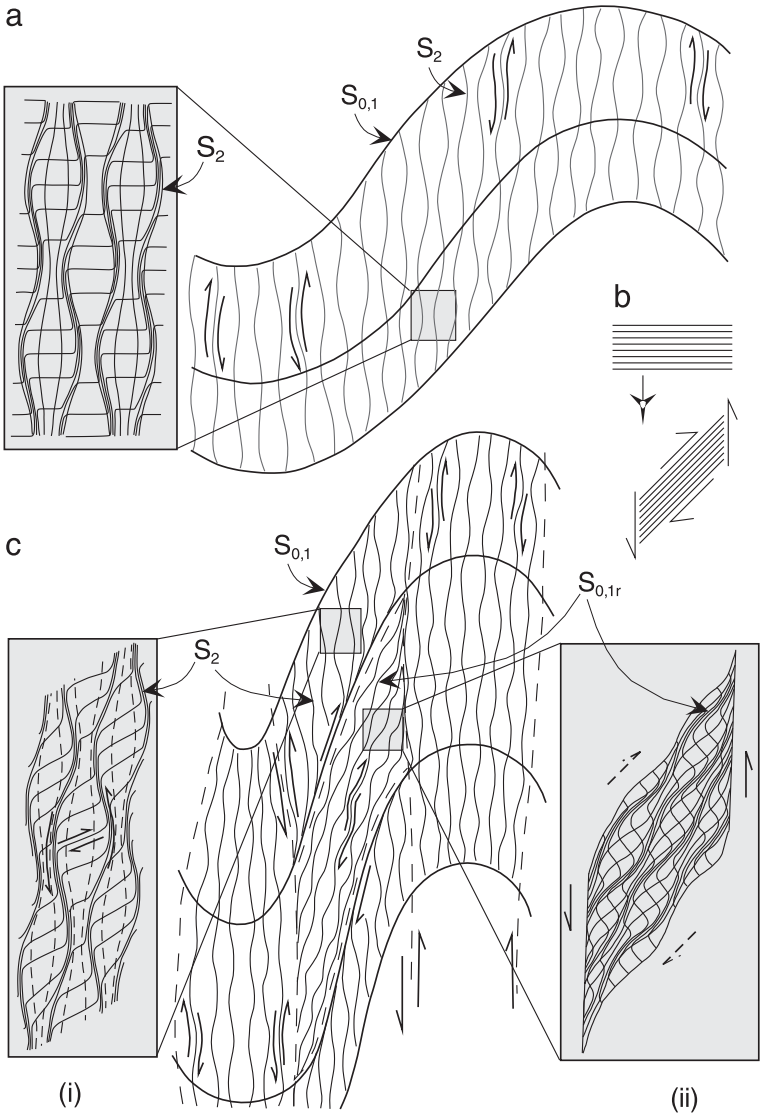

Fig. 1. (a) Limb of a fold in $S_{0,1}$ with a developing crenulation cleavage S_2. Anticlockwise shear on S_2 in as shown by arrows. There is no shear operating on $S_{0,1}$. The inset shows a strain field of a portion of this fold modeled as if it developed by progressive bulk inhomogeneous shortening (Bell, 1981). (b) Shows a card deck deformed on its boundaries by anticlockwise shear which causes the deformation to be accommodated by clockwise shear on the cards. Once the card deck has been rotated, if the bulk shear was reversed to clockwise, reactivation along the cards could no longer occur if shortening continued. Instead they would kink and perhaps gape. (c) With progressive folding, deformation becomes more non-coaxial and the fold tightens. CW reactivation of $S_{0,1}$, labeled $S_{0,1r}$, occurs contemporaneously with ACW shear along S_2. Inset (i) shows a strain field for a portion deforming by the development of a crenulation cleavage parallel to the axial plane. Clockwise shear will occur between S_2 seams on remains of S_1 as shown. Inset (ii) shows a strain field diagram where the undeformed mesh lay parallel and perpendicular to $S_{0,1}$ on the limb before reactivation began, for a portion of $S_{0,1r}$ that has reactivated.

wise shear along the cards. On a portion of the fold with an equivalent geometry to this card deck (the limb in the centre of Fig. 1a), these opposing shear senses interact and complement one another in the manner shown on this limb in the centre of Fig. 1c. They also interact at a range of scales from cren-

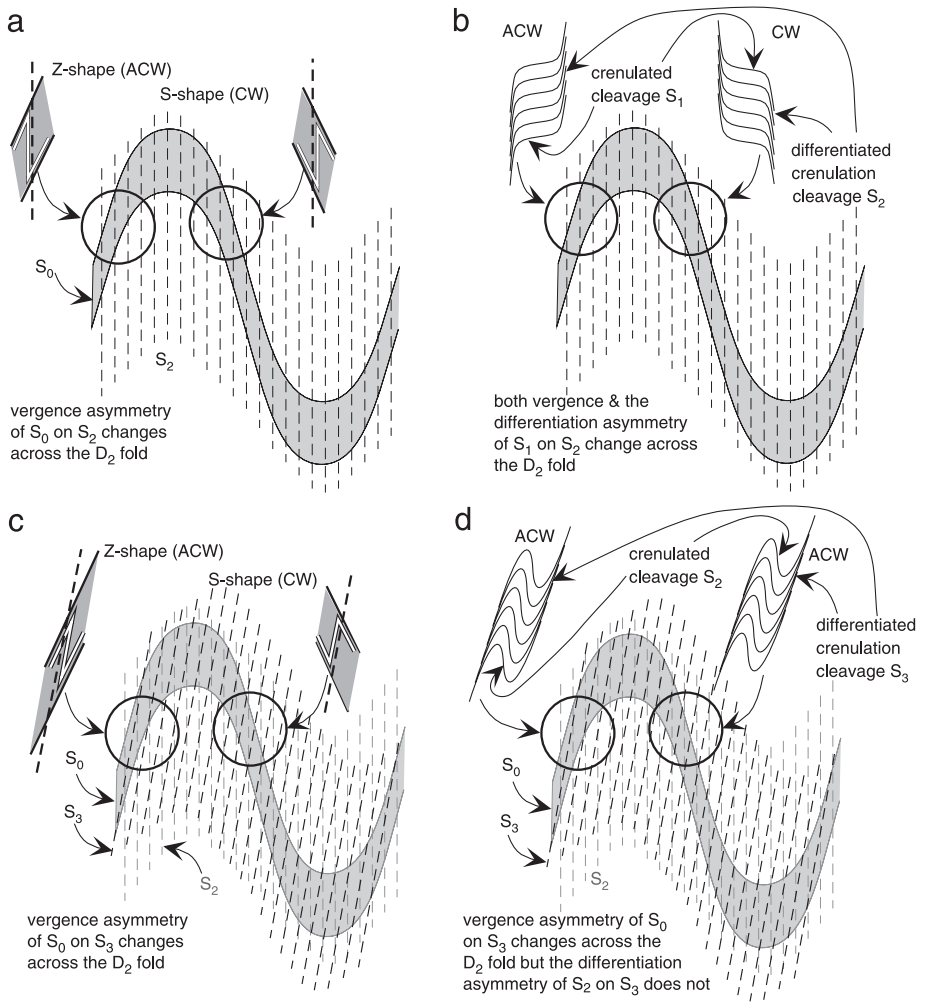

Fig. 2. A series of cross-sections showing: (a) The "vergence" asymmetry, resulting from the development of a fold synchronous with the development of an axial-plane foliation, always changes from limb to limb across a fold hinge. The Z and S bedding-cleavage relationship that helps define the "vergence" asymmetry are shown by a white outlined with black shape within the magnified portions. (b) The "differentiation" asymmetry of the S_2 cleavage that accompanied fold development in (a) changes across the fold hinge. The differentiation asymmetry is defined as the asymmetry of curvature of the crenulated cleavage (S_1 in this case) into the differentiated crenulation cleavage (in this case S_2, where is drawn as a stage 3 differentiated crenulation cleavage where the crenulated cleavage is still continuous across the differentiated cleavage seam; Bell, 1986), as shown for one crenulation hinge from each limb in the magnified portions. Significantly, the shear sense on the axial plane foliation changes across the fold hinge, (c) The D_2 fold from (a) overprinted by the effects of a younger differentiated crenulation cleavage (in this case S_3) lying at a relatively low angle to the earlier formed cleavage that formed axial plane to the D_2 fold. Note how the vergence asymmetry for S_0 on S_3 changes across the fold hinge, just as it did for the S_2 that accompanied fold development (shown in gray). If S_2 is no longer visible in the matrix, this fold would appear to have formed during D_3, and it has certainly been modified by the effects of D_3. (d) The same fold overprinted by the effects of D_3 shown in (c) but with the differentiation asymmetry of S_3 shown by the geometry of the crenulated cleavage S_2 as it passes into the differentiated crenulation cleavage S_3 as shown for one crenulation hinge from each limb in the magnified portions. Significantly, the differentiation asymmetry in this case does not change across the fold hinge because it postdated fold development. This is a very common microstructual relationship.

ulation cleavages upwards as shown in the strain field diagram in Fig. 1c (i). Above and below the portion labeled $S_{0,1r}$ in the limb of the fold shown in the centre of Fig. 1c, S_2 curves clockwise into $S_{0,1r}$ across a transition into the latter foliation along S_2 (Bell, 1986). The portion labeled $S_{0,1r}$ curves anticlockwise into S_2 across a transition into the latter foliation along $S_{0,1r}$. The strain field diagram for a portion of $S_{0,1r}$ that has reactivated is shown in Fig. 1c (ii). The process of reactivation is different from flexural flow. It can start and stop at any scale along the limb of a fold, switching back to shear along the developing cleavage, as shown in Fig. 1c. It can also start and stop at any scale across the limb of a fold, in a direction parallel to the axial plane, switching back to shear along the developing cleavage as shown in Fig. 1c. Reactivation tends to destroy parasitic folds, rather than develop them, and causes decrenulation of newly developing crenulation cleavages. All evidence that that a crenulation cleavage ever developed can be removed by reactivation, unless porphyroblast growth has occurred early in that event and preserved the crenulation hinges as inclusion trails (Bell, 1986).

2.2. Vergence asymmetry

The "vergence" asymmetry is the asymmetry of an older foliation relative to a younger one. Where a fold in bedding (S_0) and a sub-parallel foliation (e.g., S_1) develops synchronously with an axial plane cleavage (e.g., S_2, Fig. 2a), the vergence asymmetry changes across the fold as shown in the enlargements from each limb in Fig. 2a, and the crenulations change asymmetry as shown in Fig. 2b. Changes in vergence (direction to the antiform), or vergence asymmetry as described here, are routinely used to map folds and time them relative to foliations. This approach breaks down in situations such as where an upright regional fold that formed early during the deformation history (Fig. 2a) was overprinted by a younger sub-vertical foliation (S_3) with a similar strike to the axial plane as shown in Fig. 2c. S_3 changes asymmetry relative to S_0 across the hinge in the same manner as S_2 (shown in light gray), but has no genetic relationship to the fold. If the remains of S_2 have been destroyed by subsequent deformations reactivating the folded foliation (Bell, 1986), then timing the fold using the vergence asymmetry on S_3 becomes problematic. Development of S_3 will modify the fold shape, but the fold still formed in D_2.

2.3. Differentiation asymmetry

The "differentiation" asymmetry, associated with the overprinting of one foliation by another, is the asymmetry of curvature of an earlier foliation (the crenulated cleavage—S_1 in Fig. 2b) into the differentiated folia of an overprinting foliation (the differentiated crenulation cleavage—S_2 in Fig. 2b). The relationships shown in the magnified portions of each

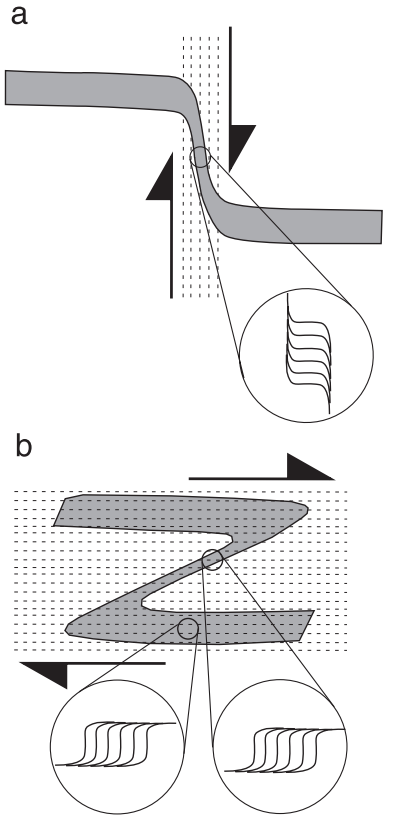

Fig. 3. Vertical schematic cross-sections showing how a fold can form by a two-stage process with a consistent asymmetry for a differentiated crenulation cleavage on both limbs. (a) First stage formed by clockwise shear accompanying the development of a vertical foliation. Enlargement shows clockwise differentiation asymmetry of the vertical differentiated cleavage. (b) Second stage formed by clockwise shear accompanying the development of a horizontal foliation. Enlargements shows clockwise differentiation asymmetry of the horizontal differentiated cleavage on all limbs.

limb in Fig. 2b are those commonly shown in textbooks (e.g., Hobbs et al., 1976), whereby the asymmetry of curvature of the crenulated cleavage, into the adjacent overprinting differentiated crenulation cleavage seam, changes across the fold hinge from anticlockwise to clockwise. In Fig. 2b, both the vergence asymmetry and the differentiation asymmetry switch across the fold hinge. However, the differentiation asymmetry in natural folds does not always change across a fold. An example of this is shown in the magnified portions of Fig. 2d, where the crenulated cleavage (S_2) maintains the same anticlockwise asymmetry into the differentiated crenulation cleavage (S_3) on both sides of the fold hinge. Thus, the vergence asymmetry in Fig. 2d has changed across the fold hinge *but the differentiation asymmetry has not changed*. Thus a fold that developed during D_2 has been modified in shape by progressive sinistral shearing and shortening associated with the development of S_3. If the remains of S_2 had been destroyed in the matrix by reactivation of S_0 (e.g., Bell, 1986, see below), but preserved in porphyroblasts, we could time this fold as having formed in D_2 because the differentiation asymmetry of D_2 inclusion trails would change across the fold. If the remains of S_2 were not preserved, we could only time this fold as having formed before or during D_3. The reason for this uncertainty in timing is that the differentiation asymmetry can explain the shape of the left limb, but not the right one. The gross orientation of the right limb would have to be the product of some earlier deformation event. A fold can form with a consistent asymmetry for a differentiated crenulation cleavage on both limbs by a two-stage process as shown in Fig. 3 (e.g., Bell and Johnson, 1992; Hickey and Bell, 2001). However, being certain of the timing of such a fold is difficult.

Thus, timing a fold relative to an "axial plane foliation" is generally straightforward where the "differentiation" asymmetry changes across the hinge but less certain where it does not. In our experience, the geometric relationships shown in Fig. 2d are commonly preserved between differentiated crenulation cleavage seams and within porphyroblasts across folds in schists (Bell and Hickey, 1997; Adshead-Bell and Bell, 1999; Hickey and Bell, 2001; Bell and Chen, 2002). However, they have rarely been described by other workers. This may have resulted from the dominance of buckling and pressure solution models for crenulation cleavage development in the 1970s and 1980s. In these models progressive shearing, during dissolution associated with cleavage development, played no role. Therefore, the asymmetry of the crenulated cleavage into the adjacent differentiated crenulation cleavage seam was considered to have little significance (Bell and Johnson, 1992).

Fig. 4. (a) Staurolite porphyroblasts preserving S_3 with a differentiated crenulation cleavage S_4 (at stage 3 of development; Bell, 1986) preserved in the matrix. S_0 dips to the west in the sample from which this photo was taken in accordance with its location on the west limb of the antiform in Fig. 5a. (b) Line diagram of photo in (a) with S_3 and S_4 labeled and showing the CW differentiation asymmetry of S_3 into S_4. Sample K25 from the west limb of antiform (Fig. 5a). Vertical section. Single barbed arrow shows strike, bearing and way up. Crossed polars. Width of base is 6 mm. (c) Shows a vertical section through a porphyroblast that has grown early during development of a horizontal crenulation cleavage in a similar manner to the staurolite porphyroblasts shown in (a) and (b). The differentiation asymmetry is clockwise and directly reflects the inclusion trail asymmetry trapped within the rim of the porphyroblast. A simple diagram that represents the trail geometry is shown. (d) Shows the porphyroblast from (c) with an extra phase of growth that occurred early during a deformation that produced a sub-vertical foliation and where the differentiation asymmetry is anticlockwise. Accumulation of the opposite asymmetry from the sub-horizontal to sub-vertical event (or vice versa) forms stair case-shaped inclusion trails within a porphyroblast. The anticlockwise differentiation asymmetry is trapped within the outer rim of the porphyroblast. A simple diagram that represents the trail geometry looks like a portion of a staircase. (e) Shows the porphyroblast from (c) with an extra phase of growth that occurred early during a deformation that produced a sub-vertical foliation and where the differentiation asymmetry is clockwise. Accumulation of the same asymmetry from a sub-horizontal to a sub-vertical event (or vice versa) forms spiral-shaped inclusion trails within a porphyroblast. The anticlockwise differentiation asymmetry is trapped within the outer rim of the porphyroblast. A simple diagram that represents the trail geometry looks like a portion of a spiral. (f) 3-D sketch of an inclusion trail through the core of a porphyroblast where the FIA changes orientation from the core to the rim from FIA 1 to FIA 2. (g) Section through the core of the porphyroblast showing three stages of growth at the core, median and rim. (h) Shows a compass with the orientations marked every 10°. Eighteen blocks of rock are cut from a horizontal slab every 10° around the compass. Vertical thin sections are cut from these blocks initially at every 30°. Extra sections are cut from blocks close to where the inclusion trail asymmetries flip. (i) Shows the asymmetry of the inclusion trails in six vertical thin sections with different strikes. The change from clockwise to anticlockwise core between the 120° and 140° sections marks the core FIA trend. The change from anticlockwise rim to clockwise rim between the 160° and 180° sections marks the rim FIA trend.

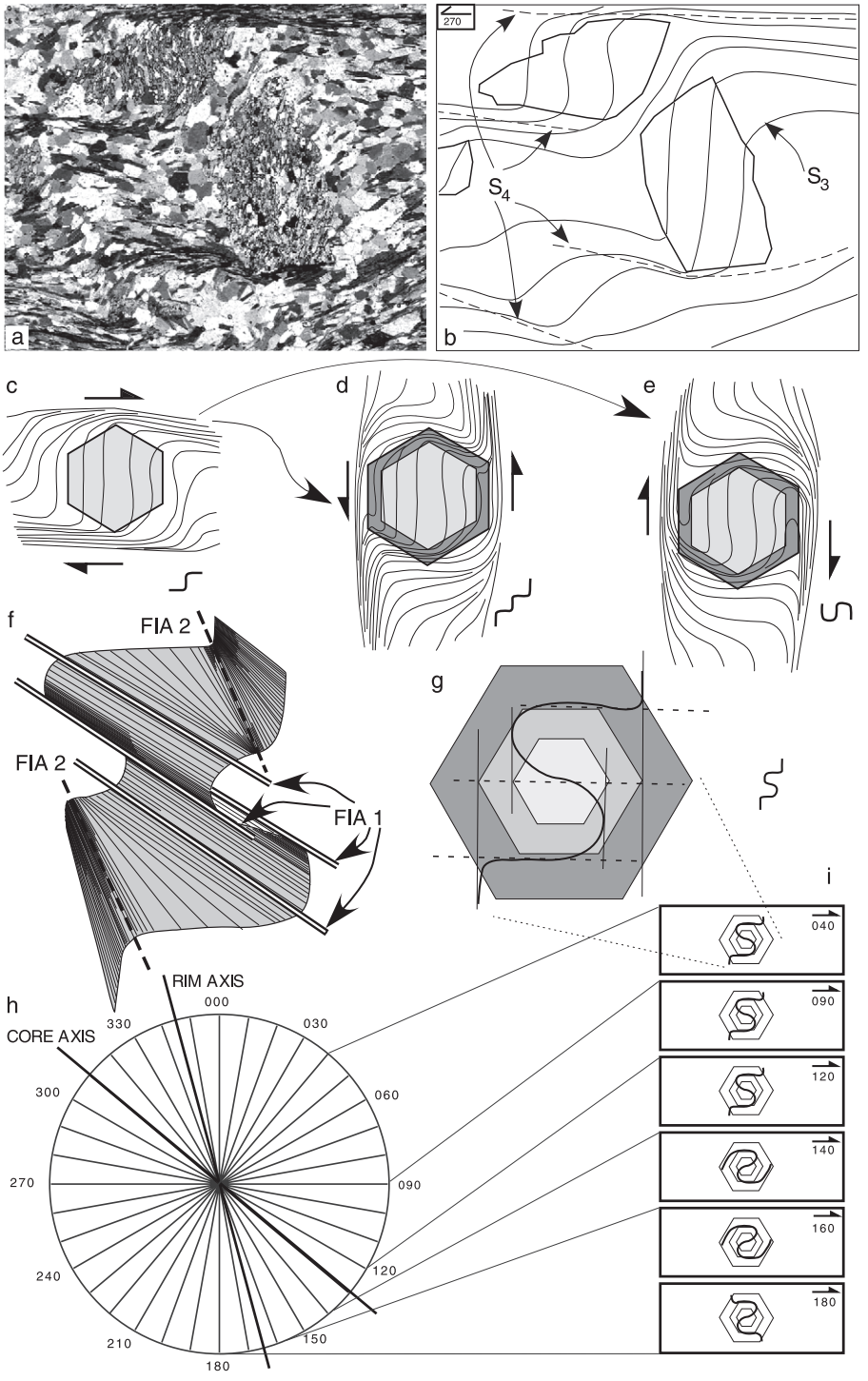
a
b
270
S4
S3
c
d
e
f
FIA 2
FIA 2
FIA 1
g
h
RIM AXIS
CORE AXIS
000
030
060
090
120
150
180
210
240
270
300
330
i
040
090
120
140
160
180

2.4. Inclusion trail asymmetry

The curvature of porphyroblast inclusion trails commonly preserves the differentiation asymmetry of one foliation into another. This asymmetry is recorded in the rim of a porphyroblast, where the inclusion trails exit into the matrix (Fig. 4a,b). We have found it to be identical to the differentiation asymmetry in the matrix where a porphyroblast grew in the same deformation event, as shown in Fig. 4a,b (Bell and Johnson, 1989, 1992; Bell and Hayward, 1991). The differentiation asymmetry is clockwise in Fig. 4a,b in the matrix, the porphyroblast and in its strain shadow. This relationship is shown with a sketch, as well as with a skeletal line diagram, in Fig. 4c. The skeletal line diagram is drawn to represent a trail passing through the centre of a porphyroblast. Fig. 4d shows a rim phase of porphyroblast growth in a younger deformation producing a crenulation cleavage with an anticlockwise differentiation asymmetry. This is preserved in the rim of the porphyroblast producing a staircase shaped inclusion pattern (shown also skeletally adjacent to the porphyroblast). If the differentiation asymmetry associated with this second crenulation cleavage had been clockwise, then the inclusion trail pattern shown in Fig. 4e would have developed instead, which has a spiral shaped skeletal pattern. Several studies have found, as shown here, that foliations preserved as inclusion trails in porphyroblasts, particularly those that are truncational, are commonly sub-vertical and sub-horizontal (e.g., Hayward, 1992; Stallard and Hickey, 2001a) and this character is visible in Fig. 4.

The preservation of the differentiation asymmetry in porphyroblasts can be applied to the timing of folds in orogens where a long history of deformation has been recorded. Studies of porphyroblast inclusion trail geometries over the past decade have revealed that the most useful way to examine inclusion trail asymmetries is to record them relative to the orientation of the foliation inflexion/intersection axis preserved within porphyroblasts (FIA). A 3D rendering of an inclusion trail surface close to the core of a porphyroblast is shown in Fig. 4f and in this example the FIA changes trend outward from core to rim. The measurement technique, described in Bell et al. (1997, 1998) and Bell and Chen (2002), and illustrated in Fig. 4h,i, allows the trend of the core and rim FIA to be measured using a radial fan of vertical thin sections. The asymmetry of the inclusion trails for the core switches between the 120° and 140° sections, constraining the trend of the core FIA. The asymmetry of the inclusion trails for the rim switches between the 160° and 170° sections, constraining the trend of the rim FIA. Success using the method shown in Fig. 4h for constraining FIA trends is dependent on a single generation of porphyroblasts not exhibiting a large variation in FIA orientation. Otherwise both anticlockwise and clockwise inclusion trail asymmetries would be recorded in every thin section within a sample. If there are multiple stages of porphyroblast growth (e.g., core-rim growth in Fig. 4g,h), any change in FIA orientation with time can be resolved (Fig. 4f–i) and even dated (Bell and Welch, 2002).

The differentiation asymmetry in porphyroblasts should be recorded at a large angle to the FIA axis on both fold limbs (e.g., Hickey and Bell, 2001). This enables the development of a regional fold to be considered relative to successive generations of porphyroblasts defined by different FIA orientations that predate the matrix foliation (e.g., Bell et al., 1998; Bell and Chen, 2002), to determine just how far back in time the fold developed. We have found that such data can provide significant information on the timing

Fig. 5. (a) Geological map of the Strathalbyn anticline (insert shows location in Australia). The anticline and adjacent syncline have near vertical axial planes and overall gently south-plunging hinges (modified from Adshead-Bell and Bell, 1999). (b) Geological map of the Bolton syncline (outlined by the Sbf and Sbc units; insert shows location in CT, USA). S_c is a composite foliation well developed on the eastern limb of the fold. Dbl Littleton Formation; Sbf and Sbc Fitch Formation and Clough Quartzite; Ogl Glastonbury Gneiss; Och and Om Collins Hill and Middletown Formations; Omo Monson Gneiss (modified from Hickey and Bell, 1999). (c) Geological map of the doubly plunging Spring Hill synform (insert shows location in Vermont, USA). The lithological units from youngest to oldest are: Yg Middle Proterozoic basement gneisses; Czh Hoosac Formation; Cr Rowe Schist; Om Moretown Formation; Ont North River Igneous Suite; Ochh hornblende amphibolite and biotite–quartz granofels Cram Hill Formation; Ochg schist and phyllite Cram Hill Formation; Ochq conglomeratic quartzite Cram Hill Formation; Ocha hornblende–plagioclase amphibolite Cram Hill Formation; Ochmc coticule Cram Hill Formation; Ochfs schist and granofels Cram Hill Formation (modified from Ratcliffe and Armstrong, 1996; Hickey and Bell, 2001). (d) Geological map of the doubly plunging Pomfret dome (insert shows location in Vermont, USA, modified from Lyons, 1955).

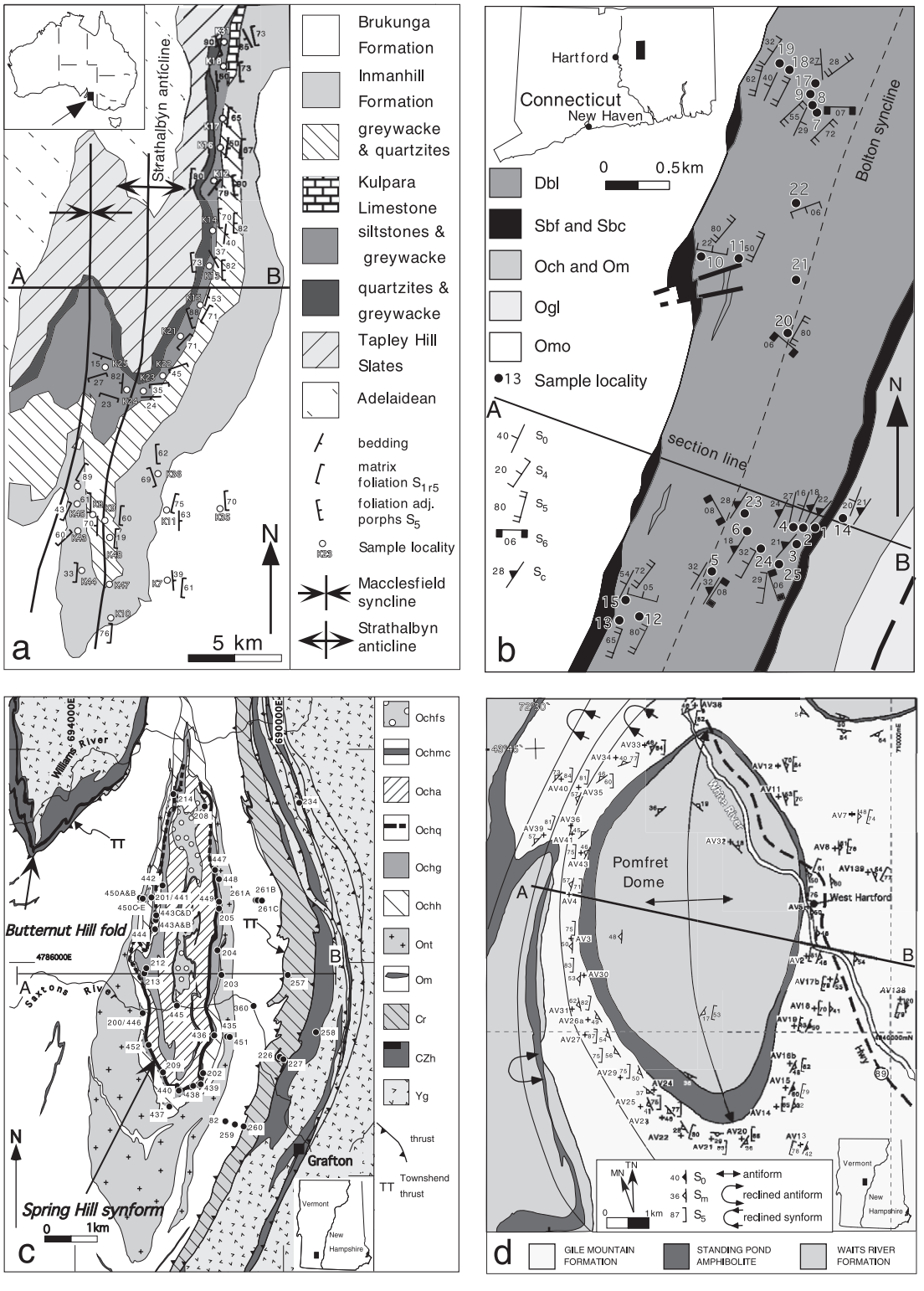
a
Strathalbyn anticline
A
B
N
5 km
Brukunga Formation
Inmanhill Formation
greywacke & quartzites
Kulpara Limestone
siltstones & greywacke
quartzites & greywacke
Tapley Hill Slates
Adelaidean
bedding
matrix foliation S1r5
foliation adj. porphs S5
Sample locality
Macclesfield syncline
Strathalbyn anticline
b
Hartford
Connecticut
New Haven
0 0.5km
Dbl
Sbf and Sbc
Och and Om
Ogl
Omo
13 Sample locality
Bolton syncline
section line
A
B
N
S0
S4
S5
S6
Sc
c
Williams River
Saxtons River
Butternut Hill fold
Spring Hill synform
TT
A
B
N
0 1km
Ochfs
Ochmc
Ocha
Ochq
Ochg
Ochh
Ont
Om
Cr
CZh
Yg
thrust
TT Townshend thrust
Grafton
Vermont
New Hampshire
d
Pomfret Dome
West Hartford
A
B
TN
MN
0 1km
S0 antiform
Sm reclined antiform
S5 reclined synform
GILE MOUNTAIN FORMATION
STANDING POND AMPHIBOLITE
WAITS RIVER FORMATION
Vermont
New Hampshire

of fold development and nappe development. It should be noted that the determination of the FIA trends and the inclusion trail asymmetry is independent of whether or not porphyroblasts rotate during growth or during subsequent deformation. The data recorded can be interpreted in the light of rotation and non-rotation models of porphyroblast growth and, in fact, used to test whether or not the porphyroblasts have rotated (e.g., Bell and Hickey, 1997; Hickey and Bell, 1999; Bell and Chen, 2002).

3. Folds that may have formed before the schistosity they fold

In the following section we describe four regional folds (Figs. 5 and 6), the first in more detail and the remaining three briefly, which fold schistosity yet are interpreted to have formed before the schistosity that they fold.

3.1. The four folds (Figs. 5 and 6)

The Strathalbyn anticline in South Australia forms a large, upright, simple macroscopic structure in Pre-Cambrian and Cambro-Ordovician rocks (Figs. 5a and 6a). The fold was thought to have formed during the third deformation event to affect the Adelaide fold belt because it folds bedding, a penetrative cleavage and a younger, oblique-to-bedding, differentiated crenulation cleavage (Offler and Fleming, 1968). However, the late timing for this fold is anomalous as adjacent, very similar, regional structures to the north and west appear to have formed much earlier as they do not fold a differentiated crenulation cleavage oblique to bedding. Adshead-Bell and Bell (1999) proposed that the Strathalbyn anticline formed very early during the deformation history, possibly at the same time as the other regional folds. They argued that the folded differentiated crenulation cleavage oblique to bedding formed during the fourth deformation event, three events after the initial development of the anticline.

The Bolton syncline in central Connecticut folds Ordovician and Siluro-Devonian rocks (Figs. 5b and 6b). Although rocks in the core of the fold are multiply deformed (e.g., Busa and Gray, 1992; Hickey and Bell, 2001), the syncline has a macroscopically simple fold geometry (Fig. 6b). However, the timing of this fold is difficult because bedding is not easily distinguished from schistosity in the field (Robinson and Tucker, 1982; Busa and Gray, 1992; Bell et al., 1997; Hickey and Bell, 1999).

The Spring Hill synform in southeast Vermont is a macroscopic fold that affects Cambro-Ordovician rocks (Figs. 5c and 6c; Ratcliffe and Armstrong, 1996; Bell and Hickey, 1997; Ratcliffe et al., 1997; Hickey and Bell, 2001). Rocks folded about this synform preserve evidence for three main phases of matrix deformation and foliation development (Hickey and Bell, 2001), and Bell and Hickey (1997) initially suggested that the fold formed after the first of these events. However, further work has shown that this timing is problematical and the fold could be much older (Hickey and Bell, 2001).

The Pomfret Dome in east central Vermont is a relatively open anticline (Figs. 5d and 6d) that has been regarded as a product of the youngest ductile deformation in the region because it folds Siluro-Devonian rocks of the Connecticut Valley Trough and the main matrix schistosity (Lyons, 1955; Ham, 2001). The rocks folded about this dome preserve evidence for three main phases of deformation and foliation development in the matrix and Ham (2001) has shown that, in a similar manner to the Spring Hill synform to the south, the late timing that has generally been accepted for this fold is problematic (see below).

3.2. Matrix foliation relationships across the folds in cross-section

Adshead-Bell and Bell (1999) showed that the differentiated crenulation cleavage S_4, lying at a low angle to bedding in the Strathalbyn antiform and thought previously to predate this regional fold, lies

Fig. 6. Cross-sections along the line AB for each of the maps in Fig. 5 with expanded insets to show details of the relationship between S_4 and S_0 on each limb of the fold. The matrix foliation labeled S_4 in each area has a form surface that is folded around the regional fold shown but dipped originally more gently than the bedding on both limbs. The vergence asymmetry of S_4 relative to S_0 suggests that S_4 formed after a fold was already present. The variation of the S_4 orientation across each fold suggests and that it has been subsequently deformed during further modification of the fold as shown in Fig. 7.

shallower than bedding on both limbs (Fig. 6a). This geometrical criterion requires that S_4 formed after the initial development of this regional fold. Looking north the differentiation asymmetry for S_4 maintains the same clockwise asymmetry shown in Figs. 4a,b and 7 across the fold. Similarly, S_3

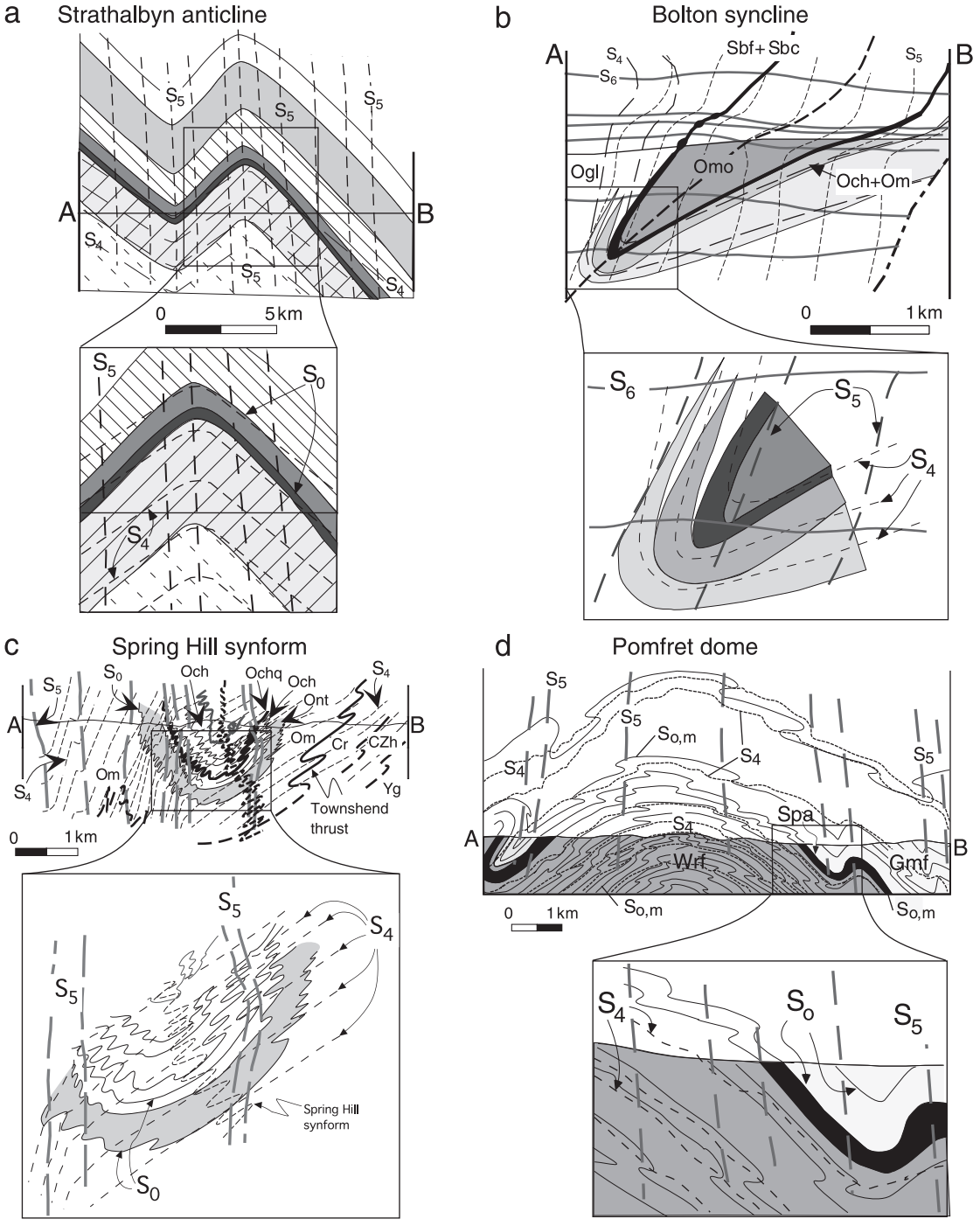

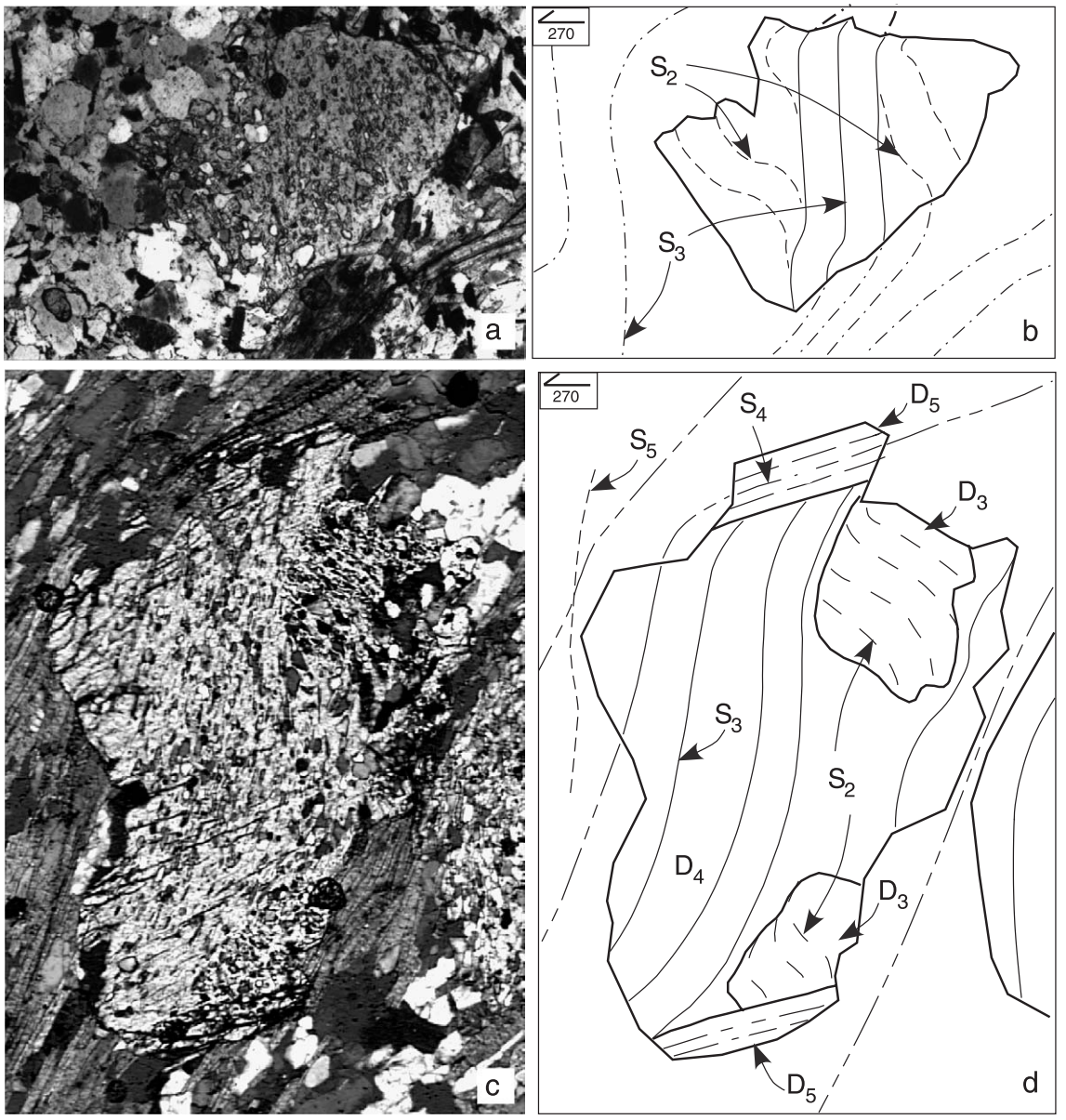

Fig. 7. (a) Staurolite porphyroblast preserving S_3 as a differentiated crenulation cleavage. (b) Line diagram of photo in (a) with S_2 and S_3 labeled and showing the CW differentiation asymmetry of S_2 into S_3. Sample K26 from the east limb of antiform due east of station K49 but off the map shown in Fig. 5a. Vertical section. Single barbed arrow shows strike, bearing and way up. Partially crossed polars. Width of base is 2.2 mm. (c) Photomicrograph of an andalusite porphyroblast exhibiting truncational microstructures and evidence for three stages of porphyroblast growth. (d) Line diagram of photo in (c) with three stages of porphyroblast growth labelled D_3, D_4 and D_5 and four foliations S_2 through S_5. The remains of the shallow foliation in the cores is S_2. The steep foliation that truncates these cores in the median is S_3. The horizontal foliation that truncates this steep foliation in the upper and lower rims is S_4. S_5 is a weakly developed crenulation cleavage in the matrix. The asymmetry of curvature of S_4 inclusion trails as they pass into the matrix is anticlockwise and probably results from the proximity of this sample to the hinge of the Strathalbyn Anticline. Most porphyroblasts in this sample show trails curving clockwise into the matrix. Sample K24. Vertical Section. Single barbed arrow shows strike, bearing and way up. Crossed polars. Width of base is 2 mm.

maintains the same clockwise differentiation asymmetry across the fold (Fig. 7; Adshead-Bell and Bell, 1999). S_5 also remains predominantly clockwise.

This same geometric relationship between S_4 and compositional layering occurs for S_4 in the Bolton syncline (Fig. 6b), the Spring Hill synform (Fig. 6c) and the Pomfret dome (Fig. 6d). However, the differentiation asymmetry for each fold is different. S_4 in the Bolton syncline, has a clockwise differentiation asymmetry looking north on both limbs (Hickey and Bell, 1999). A young, weakly developed, sub-vertical crenulation cleavage, S_5, has an anticlockwise differentiation asymmetry on both limbs. S_4 in the Spring Hill shows no overall differentiation asymmetry as the crenulated cleavage asymmetry switches back and forth relatively evenly within samples. This suggests that the deformation that produced this crenulation cleavage was essentially coaxial at the scale of the macroscopic fold (Hickey and Bell, 2001). The differentiation asymmetry for S_5 on both limbs is anticlockwise looking north. For the Pomfret dome the differentiation asymmetry for the crenulation cleavage folded around the dome, S_4, is clockwise on the west limb and anticlockwise on the east limb, as shown in Fig. 8.

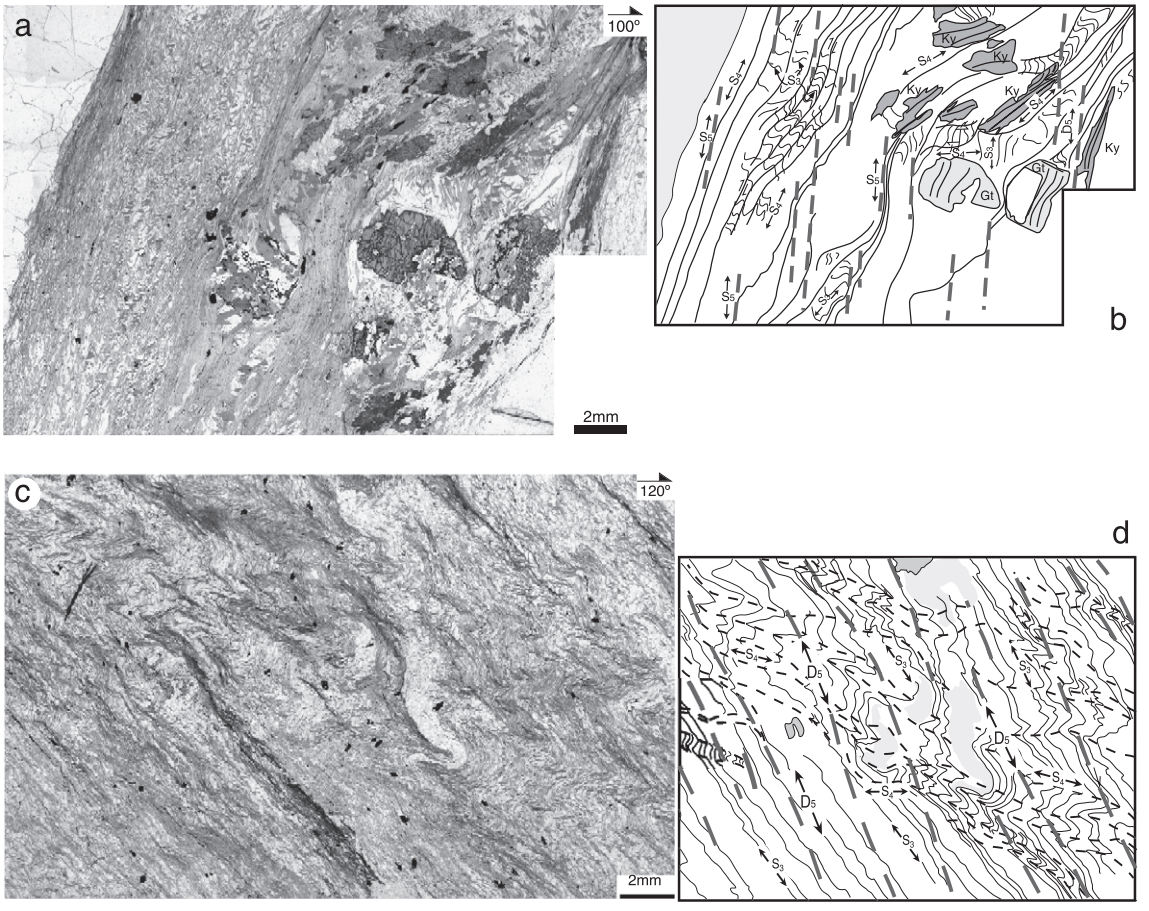

Fig. 8. Photomicrographs and line diagrams of D_4 generated differentiated crenulation cleavage S_4 on the west (a, b) and east (c, d) limbs of the Pomfret dome showing the switch in differentiation asymmetry for matrix foliations S_3, S_4 and S_5 from clockwise on the west to anticlockwise on the east. Both differentiation asymmetries are present in (c, d) but anticlockwise dominates. The compositional layering dips to the west in (a, b) and the east in (c, d) parallel to the dominant pitch of the main matrix foliation. Samples AV30 and AV15. Plane polarized light. Vertical thin sections 100° and 120°, respectively.

3.3. Porphyroblast foliation relationships across the folds in cross-section

We have recorded inclusion trail asymmetry in a manner that allows it to either be interpreted in terms of differentiation asymmetries or in terms of porphyroblast rotation. Fig. 4a,b shows a section through a porphyroblast that has grown over a crenulation hinge during the development of a sub-horizontal differentiated crenulation cleavage S_4 with a clockwise differentiation asymmetry, and preserving a sub-vertical foliation S_3. The simple skeletal sketch, shown on the bottom right of Fig. 4c, represents this clockwise asymmetry from sub-vertical to sub-horizontal. Fig. 4d shows further growth of this porphyroblast during the development of a sub-vertical differentiated crenulation cleavage with an anticlockwise differentiation asymmetry. This history of inclusion trail development is represented by a simple staircase pattern shown on the bottom right of Fig. 4d.

Fig. 4e shows the other alternative for further growth of the porphyroblast shown in Fig. 4c. This alternative involves growth during the development of a sub-vertical differentiated crenulation cleavage with an clockwise differentiation asymmetry. The simple sketch of the foliation succession shown in Fig. 4e, has a clockwise asymmetry from sub-horizontal to sub-vertical and generates a spiral outline (bottom right of Fig. 4e). Further stages of growth may accompany subsequently developed foliations preserving more steps on the staircase, spiral or some mixture of both (e.g., Fig. 4g). For every sample, each of these steps can be plotted on a histogram after separating them according to FIA trend and fold limb (see below).

Fig. 9 shows the FIA successions and trends recorded for the Bolton syncline (after Bell et al., 1997), Spring Hill synform (after Bell and Hickey, 1997) and the Pomfret dome. The succession of FIA sets 1 through 4 have been dated for the Spring Hill syncline, and remain consistent in age from sample to sample and each generation can be constrained as having begun to form prior to 424 ± 3, 405 ± 6, 386 ± 6 and 366 ± 4 Ma, respectively (Bell and Welch, 2002). Fig. 10 shows plots of the asymmetry of curvature of foliations preserved as inclusion trails in porphyroblasts, separated according to fold limb. A sketch of each fold is shown as an inset and two sets

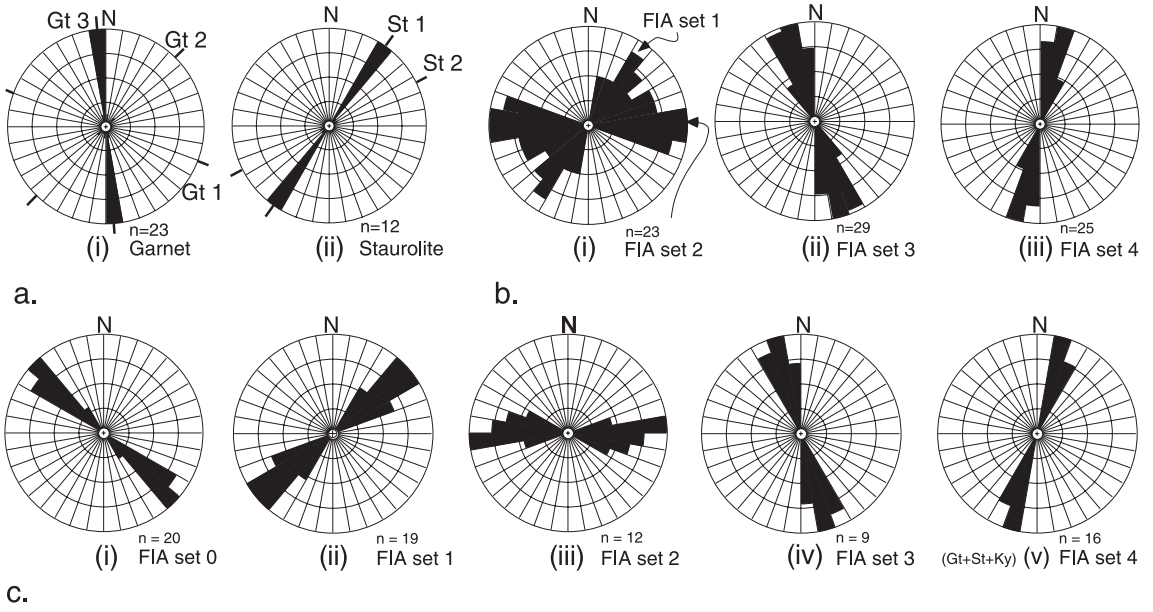

Fig. 9. Rose diagrams showing the trends of successive FIAs across the Bolton syncline (a), Spring Hill synform (b) and Pomfret dome (c). The FIA sets get progressively younger with increase in the set number.

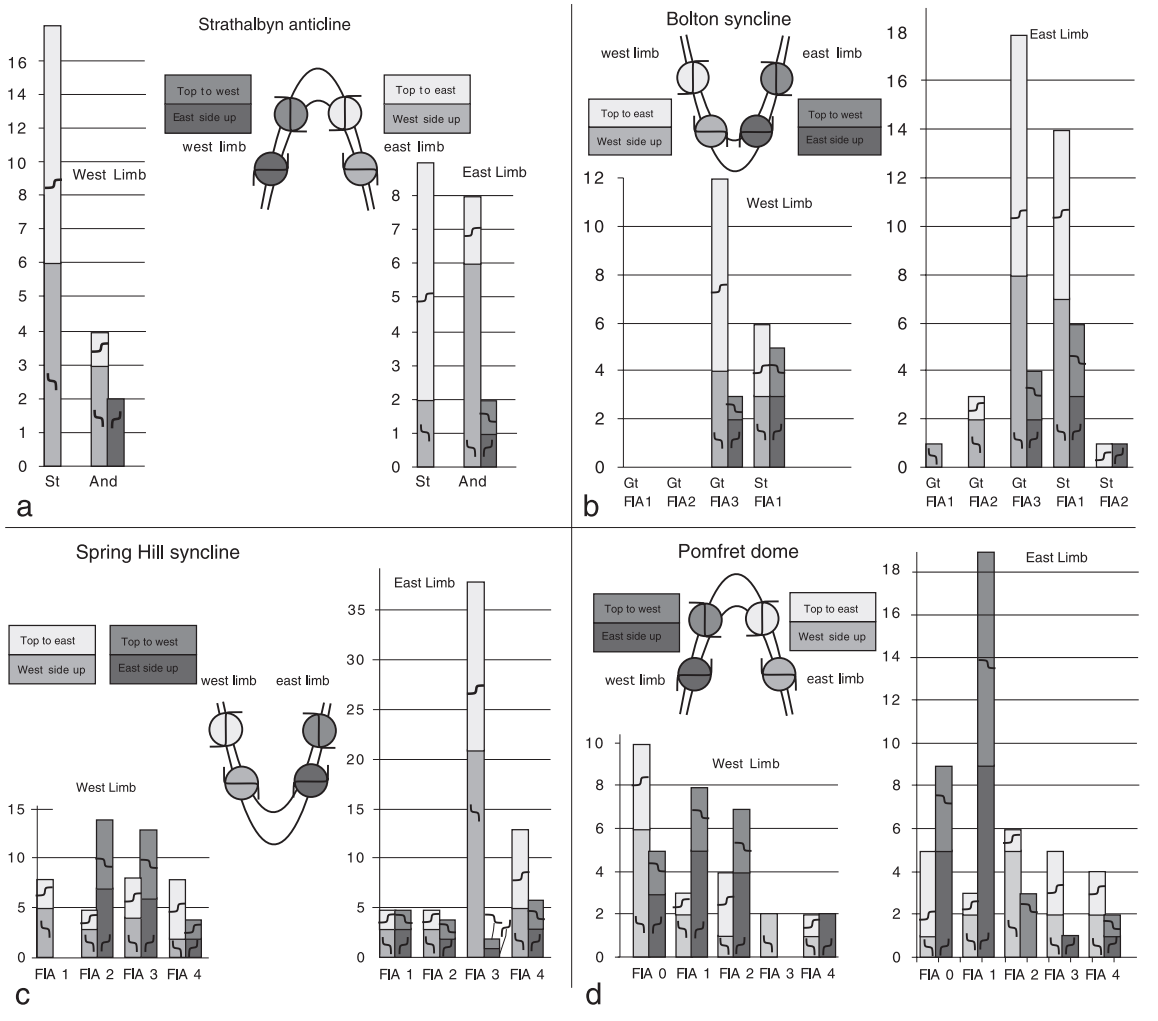

Fig. 10. Series of histograms for each limb of each fold showing the asymmetry of inclusion trails preserved within porphyroblasts. These have been separated according to whether the porphyroblasts were staurolite or andalusite in (a) and according to FIA sets in (b,c,d). Also indicated is whether the inclusion trail geometry can be interpreted as resulting from a flat-to-steep transition or a steep-to-flat transition of successive foliations. Each time the flat-to-steep or steep-to-flat succession is repeated, in a spiral or staircase-shaped trail, it is counted. This provides an indication of the amount of rotation or number of foliation events, depending on how the inclusion trails are interpreted as being formed. For each FIA set the inclusion trails asymmetry is recorded as it would project onto a W–E section when looking north with the exception of FIA 2 for the Spring Hill synform and the Pomfret Dome. These FIAs trend W–E and are viewed as looking west. FIAs 1, 2, 3 and 4 in the Spring Hill synform and Pomfret dome regions have the same SW–NE, W–E, NNW–SSE and SSW–NNE orientations, respectively. FIA 0 in the Pomfret dome region was not present in the Spring Hill synform region.

of porphyroblasts containing simple sketches of inclusion trails are drawn on each limb. The lower porphyroblasts on each limb show the flat to steep inclusion trail asymmetry, and hence differentiation asymmetry, expected for a differentiated crenulation cleavage that formed at the same time as the fold on that limb (as shown in Fig. 2b). The upper porphyroblasts show the possible asymmetries that could form during development of a sub-horizontal foliation. Each of the four possible asymmetries is shaded the same in each histogram and the asymmetry is shown within the histogram as well so that components of the histogram due to possible flat to steep or steep to flat foliation successions can be investigated.

In Fig. 10a the histograms have been marked to show whether the porphyroblasts were staurolite or andalusite. In Fig. 10b–d the asymmetries are separated according to the different FIA sets shown in Fig. 9. Fig. 10a shows that clockwise asymmetries dominate for sub vertical foliation producing vents on both limbs for the Strathalbyn anticline as well as for sub-horizontal foliation producing events. Fig. 10b shows that clockwise asymmetries dominate for sub-vertical foliation producing events for each FIA set on both limbs of the Bolton syncline except that for staurolite FIA 1, the asymmetries suggest that deformation was more coaxial on the west limb. The asymmetries for sub-horizontal foliation producing events are also predominantly clockwise. Fig. 10c shows clockwise asymmetries are dominant or equal to anticlockwise ones for sub-vertical foliation producing events on the right limb, whereas anticlockwise ones are dominant or equal to clockwise ones on the left limb with the exception of FIA set 1. The asymmetries for sub-horizontal foliation producing events are also predominantly clockwise or equal to anticlockwise ones on the right limb and anticlockwise on the left limb for FIA sets 2 and 3; clockwise dominates for FIA sets 1 and 4. Fig. 10d shows a complete mix of asymmetries but for vertical foliation producing events the asymmetries do not change across the fold in accordance with those expected for syn fold developed prophyroblasts, with the exception of FIA set 2. However, this FIA is perpendicular to the axial plane of the Pomfret dome and if the asymmetries are viewed from the opposite direction they show no relationship to the fold. Therefore, it is meaningless to consider these latter asymmetries relative to the development of the dome fold.

4. Interpretation

We interpret the development of the Strathalbyn antiform in some detail and then show how similar processes apply to the other folds.

4.1. The Strathalbyn anticline

The inclusion trails cannot be readily interpreted in terms of porphyroblast rotation because no real spiral shapes are preserved, obvious differentiated crenulation cleavages that have been helicitically overgrown are present (Fig. 7), and cross cutting differentiated cleavages are preserved in the matrix that can be correlated with the geometries preserved in the porphyroblast (Fig. 4a,b). We therefore interpret the examples of core, median and rim microstructures from the Strathalbyn anticline (e.g., Fig. 7) to indicate four phases of porphyroblast growth associated with four separate deformation events D_2 through D_5 that formed successively sub-horizontally and sub-vertically. The differentiated crenulation cleavage oblique to bedding, and thought previously to be folded by the regional fold, corresponds with the fourth of these deformation events. Because S_4 is shallower than bedding on both limbs and maintains the same clockwise differentiation asymmetry in the matrix and porphyroblasts across the fold, we interpret that it postdates initial development of the fold as shown in Fig. 11. This is supported by the differentiation asymmetry for the vertical crenulation cleavage S_5. Although S_5 lies sub-parallel to the axial plane to the fold, the differentiation asymmetry remains clockwise across the hinge. Indeed, the inclusion trail asymmetries remain predominantly clockwise, looking north,

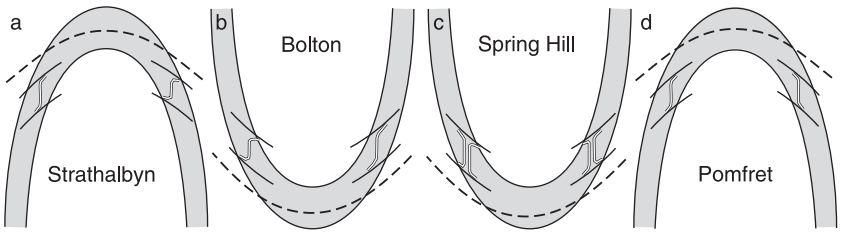

Fig. 11. Schematic cross-sections of the Strathalbyn anticline (a), Bolton syncline (b), Spring Hill synform (c) and Pomfret dome (d). These folds are drawn as upright folds with the effects of younger deformations removed. This enables the vergence asymmetry (dashed lines) and differentiation asymmetry (black outlined white lines = crenulated cleavage, solid lines = differentiated crenulation cleavage) can be readily compared, from area to area, for the folded matrix foliation that is locally oblique to compositional layering.

for all phases of porphyroblast growth on both limbs (Fig. 10a). Consequently, there is no record of the timing of fold development preserved by the inclusion trail asymmetries within the porphyroblasts.

We interpret this to indicate that the initial macroscopic fold formed prior to porphyroblast development during D_1. Fig. 12, modified from Adshead-Bell and Bell (1999), shows how the fold initially developed by horizontal shortening during D_1 (Fig. 12a), with the formation of a sub-vertical axial-plane cleavage, S_1. Porphyroblast growth commenced early during D_2 when development of sub-horizontal S_2 occurred due to vertical shortening accommodated by flattening/volume loss plus a component of dextral shear (single barbed arrows). S_2 transected the D_1 fold and rotated the right limb to a steeper orientation, and the left limb to a shallower orientation, as shown in Fig. 12b (differentiation asymmetry shown in the enlargement). Development of sub-vertical S_3 during horizontal shortening with a component of dextral shear (shown by single barbed arrows) occurred during D_3 (Fig. 12c). S_3 formed sub parallel to the axial plane to the fold and rotated the right limb to a steeper orientation and the left limb to a slightly shallower orientation, although this rotation would have been opposed by volume loss accompanying foliation development. S_2, folded by the effects of D_3, is shown as a dotted line. The differentiation asymmetry is the same on both limbs (see enlargement in Fig. 12c). Reactivation of S_0 on the right limb will rotate S_2 towards the bedding faster than shear on S_3 will rotate S_0 towards the axial plane (see below). Development of sub-horizontal S_4 during vertical shortening plus a component of dextral shear (shown by single barbed arrows) occurred during D_4 (Fig. 12d). S_4 transected the fold and rotated the right limb to a steeper orientation and the left limb to a shallower orientation. Reactivation of S_0 on the left limb will rotate S_2 and S_4 towards the bedding faster than shear on S_4 will rotate S_0 away from S_4 on the right limb (see below). Development of sub-vertical S_5 during horizontal bulk shortening plus a component of dextral shear (shown by single barbed arrows) occurred during D_5 (Fig. 12e). S_5 formed sub

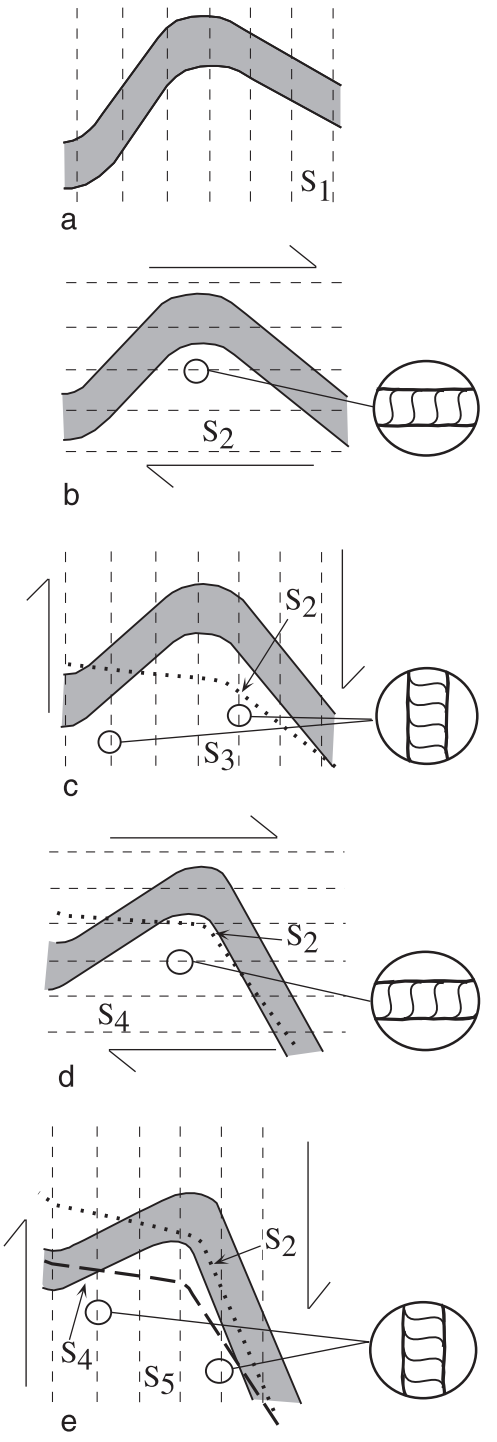

Fig. 12. Series of sketches showing the interpreted progressive development of the Strathalbyn anticline during five orthogonal foliation-producing deformation events (see text for a detailed explanation).

parallel to the axial plane to the fold and rotated the right limb to steeper orientation and the left limb to a slightly shallower orientation although this rotation was partly opposed by syn-deformational volume loss. S_4 is shown with a heavy dashed line folded by the effects of D_5. The differentiation asymmetry is the same on both limbs (see enlargement in Fig. 12e). Reactivation of S_0 on the right limb will rotate S_4 towards the bedding faster than shear on S_5 will rotate S_0 towards the axial plane (see below).

We interpret that reactivation of pre-existing foliations (Fig. 1) plays a very significant role in both the rotation and decrenulation of developing crenulation cleavages and this is shown in Fig. 13. Reactivation varies with the competency contrast between the layers. Where compositional layering is suitably oriented for reactivation to begin from the commencement of a new deformation event, the more competent layers appear to deform more readily by reactivation and the weaker ones tend to commence deformation by crenulation. However, locally the weaker layers deform by reactivation from the commencement of deformation. Any foliation that forms with a sub-horizontal orientation across the fold, such as S_2 and S_4 in the Strathalbyn anticline, will tend to be rotated towards the folded compositional layering by the effects of synchronous reactivation as well as subsequent horizontally directed shortening. Fig. 13a shows a schematic representation of the Strathalbyn antiform. The clockwise looking north differentiation asymmetry on S_4 resulting from non-coaxial shortening and shearing will cause developing D_4 crenulations to unfold (Fig. 13b) on the left limb and any remains of S_4 to be rotated towards S_0 as shown in Fig. 13c. S_4 will continue to develop on the right limb (Fig. 13d,e) because S_0 is not in an orientation that is suitable for reactivation. However, during D_5, S_4 on this limb will be rotated towards S_0 by the effects of horizontal shortening. Similar behaviour would have occurred in D_2 followed by D_3.

The multiple phases of porphyroblast growth track the P–T path that the rocks pass through from D_2

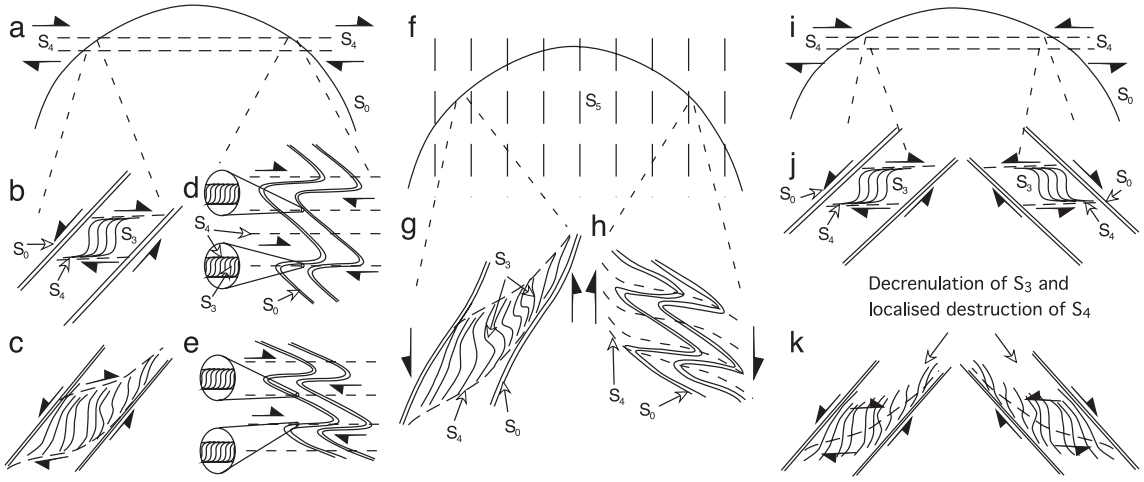

Fig. 13. Cross-sectional sketches looking overall towards the north. (a) Schematic of the upright Strathalbyn antiform showing the effects of developing a sub-horizontal S_4 with a clockwise differentiation asymmetry (shown by the single barbed arrows). (b) On the left limb, anticlockwise reactivation of S_0 can occur and will accommodate some of the effects of clockwise shearing on S_4. (c) Such reactivation results in decrenulation of D_4 crenulations and thus unfolding and rotation of S_3 towards S_0. Remains of S_4 are also rotated towards S_0. (d) On the right limb, reactivation of S_0 is not possible (see caption for Fig. 1b), and S_4 continues to develop as a crenulation cleavage. (e) Continued deformation leads to intensification of the S_4 cleavage. (f) Shows horizontal shortening of a fold such as that in (a). (g) Shows the rotational effects on S_4 relics on the left limb where the differentiation asymmetry is anticlockwise (this is not the case in the Strathalbyn anticline (see Fig. 12e) but is the case for the Bolton synform, the Spring Hill synform and Pomfret dome). (h) Shows the effects on the right limb where the differentiation asymmetry is clockwise, which is the case for the Strathalbyn anticline. (i) Shows a schematic of the Pomfret dome where the differentiation asymmetry on S_4 switches across the fold as shown. (j) Shows that reactivation of S_0 can occur on both limbs of the dome fold synchronous with D_4 development. (k) Shows the effects of reactivation of S_0 causing decrenulation and rotation of S_3 towards S_0 plus rotation of the remains of S_4 towards S_0.

through D_5. Because both andalusite and staurolite porphyroblasts commonly grow together in the same sample, the path followed is well constrained in P–T space and this was described by Adshead-Bell and Bell (1999). The degree of modification of the fold shape during the development of these younger foliations is uncertain because the amount of volume loss during the formation of each successive differentiated crenulation cleavage is unknown. Since each deformation is taken up by a combination of shortening and shear, with a lot of the apparent shear being accommodated by volume loss, the degree of modification of the fold shape need not be great. Reactivation of the compositional layering that defines the fold may help result in minimal modification of the fold shape. Bell (1986) showed microstructures associated with reactivation that suggest more significant volume loss occurs during this process than during differentiated crenulation cleavage development.

4.2. The Bolton syncline, Spring Hill synform and Pomfret dome

A developing sub-horizontal foliation cross cutting an upright fold (called S_4 in all three areas) can maintain the same differentiation asymmetry (Fig. 11a,b) or switch it from limb to limb (Fig. 11d). If the same differentiation asymmetry is maintained as shown in Fig. 13a, then compositional layering on one limb of the fold can reactivate (Fig. 13b,c), but not on the other (Fig. 13d,e). Where reactivation can occur, developing D_4 crenulations of S_3 in Fig. 13 will tend to decrenulate, S_4 will tend to be destroyed and S_3 will be rotated towards S_0 (Figs. 1 and 13c). Any remains of S_4 in layers less affected by reactivation will also tend to be rotated towards S_0. Where reactivation cannot occur (see caption to Fig. 1b), the S_4 crenulation cleavage will continue to develop (Fig. 13d) and intensify with further deformation (Fig. 13e). Subsequent horizontal shortening (Fig. 13f) can further rotate S_4 towards S_0 (Fig. 13g,h). Combined, these processes will give the originally gently dipping foliation a folded appearance that suggests the fold developed later than the foliation. If the differentiation asymmetry switches across the fold hinge in the manner recorded at the Pomfret dome (Figs. 11d and 13i), then reactivation of both limbs of the dome fold is possible (Fig. 13j) and D_4 crenulations will tend to decrenulate (Fig. 13k) with earlier foliations being rotated towards S_0 and any remains of S_4 doing the same. The interpretations shown in Figs. 12 and 13 suggest that all four of the regional folds were formed before the folded crenulation cleavage that is locally oblique to the compositional layering.

4.3. Differentiation asymmetry in porphyroblasts and timing of the regional fold

We have shown in Fig. 4a–c how the asymmetry of curvature of foliations defining crenulated cleavages, where preserved as inclusion trails in porphyroblasts that are continuous with matrix foliations, reflect the differentiation asymmetry formed in synchronously crenulated matrix developed to stage three of crenulation cleavage development (Bell, 1986; Bell and Hayward, 1991). Therefore, if porphyroblasts preserve a very long history of foliation development as a succession of inclusion trail development, the history of differentiation asymmetry is preserved as well. Bell and Welch (2002) have shown that the succession of FIAs preserved from core to rim in porphyroblasts around the Spring Hill synform can be dated and remains consistent in the five (the fifth sample was dated recently, Welch and Bell, unpublished data) samples dated with multiple FIAs for the same FIA set. Indeed they showed that up to 75 million years of history is preserved inside the porphyroblasts that has been completely obliterated from the matrix. Consequently, we are confident that the differentiation asymmetry can be interpreted for all the successive deformations trapped as inclusion trails within the porphyroblasts (Fig. 4d,e) and separated in time according to the succession of FIA trends (Figs. 4f–i and 9) as shown in Fig. 10. The fact that consistent FIA successions are preserved from sample to sample across large regions (Bell et al., 1998), have shallow plunges (Bell and Hickey, 1997; Hickey and Bell, 1999) and give consistent ages for each FIA set in the Spring Hill anticline (Bell and Welch, 2002), cannot be explained via a model that involves porphyroblast rotation.

Each fold examined in this study shows both asymmetries on both limbs for shallow to steep or steep to shallow overprinting foliations separated according to the FIA succession (Fig. 10b–d). Where the same asymmetries accumulate from shallow to

steep and steep to shallow events, spiral-shaped inclusion trails develop (Fig. 4c,e). If they switch back and forth, staircase shaped trails develop (Fig. 4c,d). For each fold, there are no consistent inclusion trail asymmetry switches for any FIA set that can explain the initial development of both limbs. The actual asymmetry that should develop on each limb is shown on the sketch of each fold in Fig. 10 using porphyroblasts where the trails switch from flat in the core to steep on the rim (the lower two porphyroblasts in each case).

Both asymmetry trails, for many of the FIA sets on both fold limbs in Fig. 10, suggests that for many periods of porphyroblast growth the deformation was essentially coaxial at the bulk scale. Commonly, the set that does not accord with that related to the appropriate fold limb (lowermost porphyroblasts sketched on each fold inset), dominates. This suggests that the development of all the inclusion geometries observed, including spiral-shaped ones, is related to some process that affects each limb differently, rather than a product of rotation of the porphyroblasts in a shear zone (e.g., Stallard and Hickey, 2001b; Bell and Chen, 2002) and this is discussed in some detail below. Since we could find no asymmetry switches that match those expected to accompany fold development, we argue that each fold predated all porphyroblast growth.

For some periods of porphyroblast growth, one asymmetry is strikingly dominant on one limb. This is particularly the case for the Bolton syncline, Spring Hill synform and Pomfret dome, but less so for the Strathalbyn anticline. These asymmetries are those for garnet FIA 3 and staurolite FIA 1 from the East limb of the Bolton syncline (Fig. 10b), FIA 4 and FIA 5 on the east limb of the Spring Hill synform (Fig. 10c), FIA 2 on the east limb of the Pomfret dome (Fig. 10d), and the first asymmetry set on the west limb of the Strathalbyn anticline (Fig. 10a). Interestingly, the dominant asymmetry is always on the limb where the shallow to steep asymmetry is the opposite to that expected for a fold associated with the development of that limb. For example, the flat to steep asymmetry histogram for FIA 3 on the east limb in Fig. 10c is the asymmetry expected for the left limb (shown in the lower sketch of a porphyroblast on this limb of the fold inset) and much bigger than the asymmetry expected for this limb.

Fig. 14 shows a fold similar to that in Fig. 2c, d where the differentiation asymmetry for the cleavage developed parallel to the axial plane is anticlockwise on both limbs of the fold. The anticlockwise shear sense on the axial plane cleavage is such that the folded compositional layering on the left limb can reactivate by antithetic shear relative to the axial plane cleavage as shown in Fig. 1b,c (Bell, 1986) and the possible resulting geometries are shown in the insets. Because the cleavage forming parallel to the axial plane postdates this fold, the left limb has an orientation that allows reactivation of the compositional layering to occur from the commencement of deformation. This reduces the amount of rock on this limb that undergoes crenulation and diminishes the sites where the development of a new crenulation cleavage can occur. We argue below that this would reduce the number of porphyroblast growth sites on this limb as we have suggested previously that porphyroblasts nucleate in zones of progressive shortening (Bell et al., 1986). However, the shear sense on the axial plane cleavage, on the right limb of the fold shown in Fig. 14, is not synthetic to the fold and the folded compositional layering cannot reactivate, as described for Fig. 1b. Consequently, this limb keeps on deforming through the development of a crenulation cleavage. We argue below that this provides more sites for porphyroblast nucleation and growth and explains the common development of more porphyroblasts with the opposite asymmetry to that expected classically and shown on the fold insets in Fig. 10.

4.4. Fold development for the Bolton synform, Spring Hill synform and Pomfret dome

As argued above, the three folds are interpreted to predate the oldest visible matrix foliation for which we can determine a differentiation asymmetry because this foliation has a gently dipping enveloping surface that cuts both limbs with the wrong vergence as shown in Figs. 4a and 8 and summarized in Fig. 11. The three folds predate the foliations preserved as inclusion trails within porphyroblasts as discussed above (Fig. 10). Inclusion trails that develop within porphyroblasts during fold development should switch asymmetry across an antiform or synform fold hinge in the manner shown for the lowermost por-

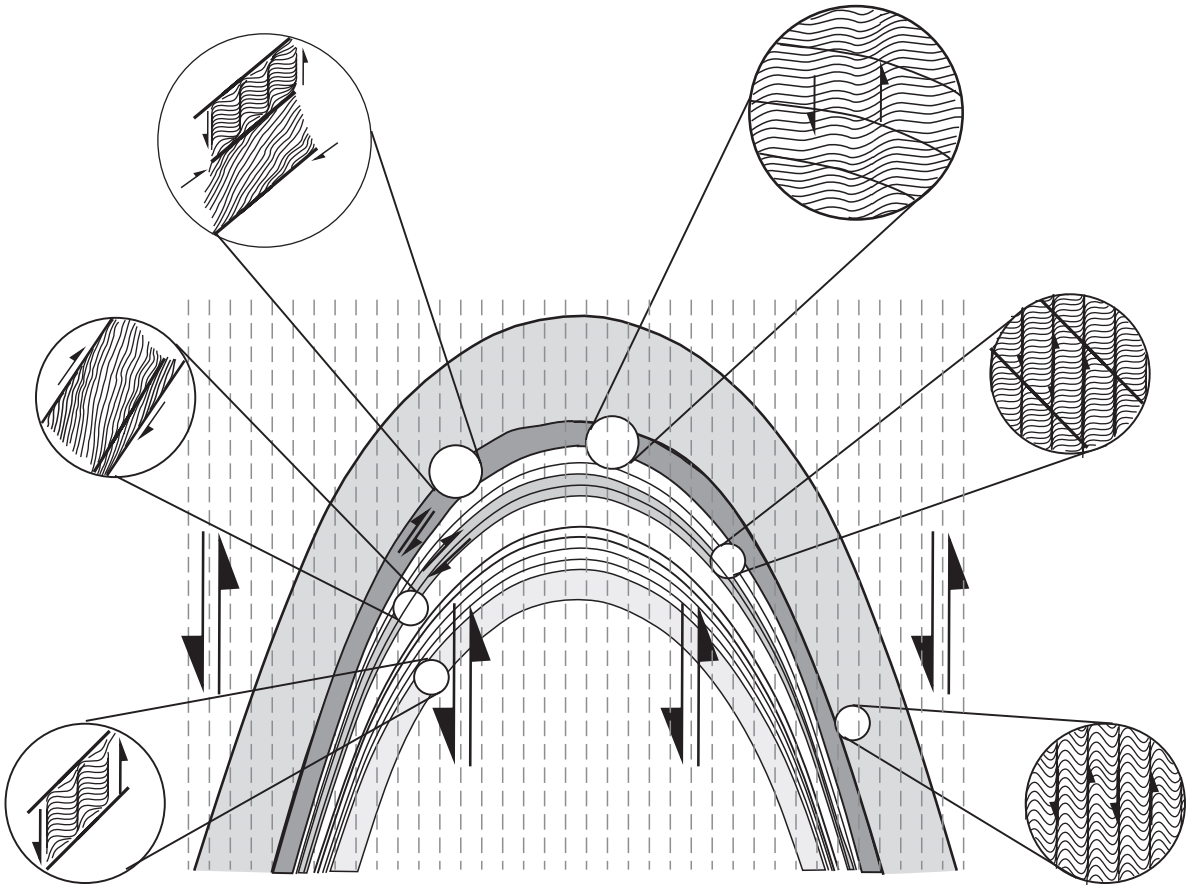

Fig. 14. Sketch showing anticlockwise shear operating on a sub-vertical axial plane cleavage on both limbs of a fold (large single barbed arrows) that was previously overprinted by a sub-horizontal foliation (visible in the crenulation hinges of the magnified portions). Beds on the left limb can reactivate from the commencement of deformation but those on the right limb cannot. This is shown by the clockwise shear senses within two of the beds (small single barbed arrow). Moving clockwise around the left limb the insets show development of an axial plane crenulation cleavage, reactivation with no crenulation cleavage development, and a transition between the two. Porphyroblasts nucleate in crenulation hinges at the commencement of the crenulation deformation event (Bell and Hayward, 1991) and cease growing once stage 3 of crenulation cleavage development is reached. On the right limb, reactivation of the bedding cannot occur from the commencement of deformation. The deformation of the previously formed sub-horizontal foliation is everywhere more coaxial at the commencement of deformation, providing more sites for porphyroblast nucleation, before differentiated crenulation cleavage develops.

phyroblasts on the fold insets in Fig. 10. This is not the case for any of the folds described herein. Clockwise asymmetries dominate on both limbs of the Strathalbyn anticline (Fig. 10a) and the Bolton syncline (Fig. 10b) suggesting that none of the history of deformation preserved within the porphyroblasts relates to fold development (e.g., Fig. 12). Both asymmetries for each FIA set are relatively abundant on both limbs of the Spring Hill synform except those for FIA 4, which show a dominance of clockwise asymmetries on the east limb and anticlockwise on the west limb and clockwise asymmetries dominate on both limbs for FIA 5 (Fig. 10c). None of this history relates directly to fold development. Fig. 10d shows that both asymmetries are relatively abundant on both limbs of the Pomfret dome, except for FIA 2 where there is a dominance of anticlockwise asymmetries on the east limb and a less significant dominance on the west limb. For FIA 4, there is dominance of clockwise asymmetries on both limbs.

Consequently, none of this history relates directly to fold development.

We conclude that these three regional folds, as did the Strathalbyn anticline, formed before porphyroblast growth began, but were progressively and extensively modified by subsequent deformations. We cannot preclude for all cases the possibility that some of the folds formed by a two stage process as shown in Fig. 3. However, we feel that we can preclude it for the Strathalbyn anticline and the Bolton syncline. The anticlockwise asymmetry from a sub-horizontal to a sub-vertical foliation required to form the west and east limb of these two folds, respectively, never dominate the relevant limbs (Fig. 10a and b) and, therefore, these limbs must have developed prior to porphyroblast growth. We showed in Fig. 12 how the overprinting of predominantly clockwise shear during the development of successive sub-vertical and sub-horizontal foliations can modify but preserve a pre-existing fold shape. For the Spring Hill synform, anticlockwise asymmetries from sub-horizontal to sub-vertical equal clockwise asymmetries on the east limb for FIA 1, but are never dominant or equal for any of the other FIA sets (Fig. 10c). Therefore, this limb may have formed during the development of FIA 1. For the Pomfret dome, the west limb can have formed during the development of FIA 2 when the anticlockwise asymmetry from a sub-horizontal to a sub-vertical foliation required to form it was dominant (Fig. 10d). Similarly, the east limb can have formed during the development of FIA 4 or 5 when the clockwise asymmetry from a sub-horizontal to a sub-vertical foliation required to form it was dominant (Fig. 10d).

5. Discussion

5.1. Porphyroblast rotation versus sub-horizontal and sub-vertical directed bulk shortening

Porphyroblast rotation accompanied by the development of spiral-shaped inclusion trail geometries has been attributed to the development of highly non-coaxial shear zones (Williams and Jiang, 1999). Such shear zones should be through going structures that cut across or are folded by the regional folds described herein. If this had occurred, at least one of the FIA sets, for the asymmetric inclusion trails shown in Fig. 10, should preserve consistent asymmetries across the fold as all preserve some spiral-shaped inclusion trails. Even if one argued that all early-formed porphyroblasts were being rotated as the youngest ones formed, the youngest ones should show a consistent asymmetry across the fold, but this is not the case. Significantly, the trend of successive FIA sets (Fig. 14) remains very consistent across these folds (Bell and Hickey, 1997; Bell et al., 1997; Hickey and Bell, 1999; Ham, 2001) as well as regionally (Bell et al., 1998). Furthermore, the plunges of each FIA set remain sub-horizontal (Bell and Hickey, 1997; Hickey and Bell, 1999). These authors concluded that these data demonstrated that the porphyroblasts had not rotated, relative to geographic coordinates or with respect to the vertical, during or after the ductile deformation that accompanied or postdated porphyroblast development. This is strongly supported by the dating of the FIA sets using monazite inclusions, which has revealed ages that are consistent from sample to sample for the same FIA sets (Bell and Welch, 2002).

The variation in inclusion trail asymmetry across the folds shown in Fig. 10 is consistent with a model of porphyroblast non-rotation, but is not obviously so for a rotation model. If porphyroblasts nucleate in crenulation hinges and record the asymmetry associated with a developing crenulation cleavage, then successions of weakly developed cleavages forming against porphyroblast rims can preserve spiral-shaped inclusion trail geometries such as those recorded in the succession from Fig. 4c to e, or staircase inclusion geometries such as those recorded in the succession from Fig. 4c to d. Normal heterogeneous deformation associated with fold development and subsequent modification of that fold by further deformation, rather than extensive shear zone development, can produce the range of geometries recorded in Fig. 10.

Futhermore, where one set of asymmetries dominates, the other asymmetry is generally present (Fig. 10b Gt FIA 3 and St FIA 1, Fig. 10c FIA 3 and 4, Fig. 10d FIA 1 and 2). The frequency of phases of growth of porphyroblasts that preserve the dominant asymmetry, is greater on one limb than the other. This variation can be explained if they formed by succes-

sive overprinting of sub-vertical and sub-horizontal foliations, but is inconsistent with models of porphyroblast rotation. Both asymmetries of inclusion trails (including spiral-shaped trails) are common on both limbs for most FIA sets for the Bolton, Spring Hill and Pomfret folds. This relationship can be more readily explained by successive overprinting of near-orthogonal foliations due to overall coaxial deformation, rather than the complex scenarios of forwards and backwards rotation required by porphyroblast rotation models.

5.2. The early development of regional folds

We suggest that the early development of the regional folds examined herein, plus the younger development of the matrix schistosity that they fold, will prove to be a common feature of orogenic belts. Successions of sub-vertical and sub-horizontal foliations are difficult to recognize in the matrix of multi-deformed rocks because the youngest event tends to rotate the foliations developed in earlier events. However, recently, such successions have been shown to have occurred in several areas (e.g., Aerden, 1994, 1996, 1998; Bell and Hickey, 1998). Successions of sub-vertical and sub-horizontal foliations are commonly recognized in porphyroblasts in many orogens (e.g., Johnson, 1990; Hayward, 1992; Davis, 1993; Aerden, 1994, 1998; Jones, 1994). Such overprinting of multiple successive sub-vertical and sub-horizontal foliations as that suggested by the foliations preserved in porphyroblasts increases the heterogeneity of deformation within an originally planar sedimentary package with each successive event (Fig. 15). Consequently, the best opportunity for the development of large wavelength and amplitude upright folds occurs during the first phase of horizontal shortening to affect a sedimentary package (Fig. 15a). Heterogeneous partitioning of vertical shortening due to gravitational collapse (Elliot, 1976; Bell and Johnson, 1989; Jones et al., 1996; Royden, 1996; Rey et al., 2001) will tend to cut sub-horizontal zones of high strain across these vertical folds (Fig. 15b) increasing the heterogeneity of the rock package. Renewal of the effects of horizontal shortening is expected to produce either smaller wavelength folds or to amplify the remains of earlier developed ones as shown in Fig. 15c. Repetition of this deformation succession will further increase the heterogeneity of the rock package, decreasing the size of any folds that nucleate for the first time.

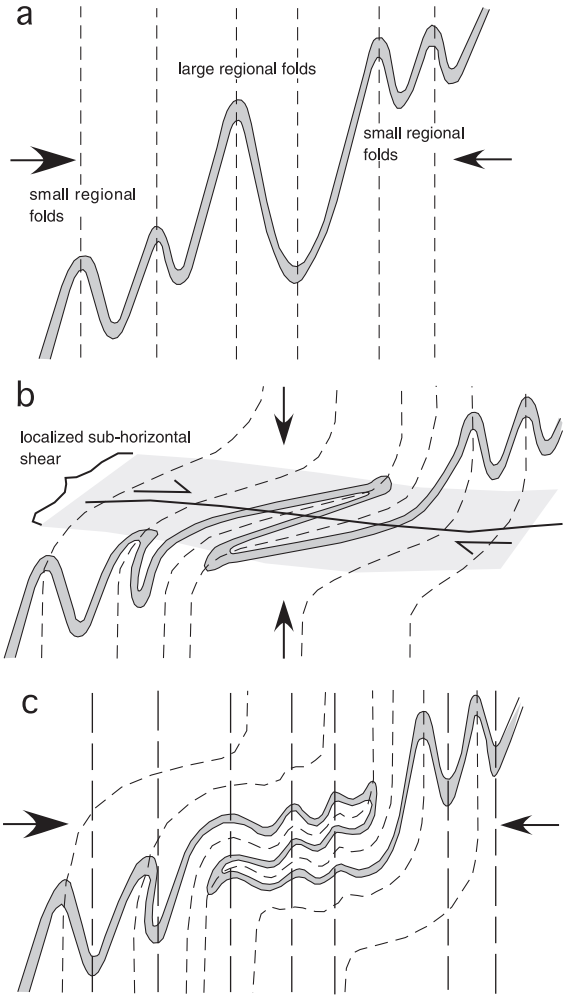

Fig. 15. A series of sketches of cross-sections showing how the large regional folds in (a) can be progressively reduced in size and modified in shape by successive sub-vertical (b) and sub-horizontal directed shortening (c). Note in (c) that if there is no change in the direction of horizontal shortening, the same cleavage continues to develop in regions unaffected by horizontal shear. With each repetition of localized sub-horizontal shear during sub-vertical shortening, especially on more closely spaced zones, the folds are reduced in amplitude. Each intervening episode of horizontal shortening increases the amplitude of un-rotated portions of the original folds and creates new folds in rotated portions as shown in (c). The new folds tend to have smaller amplitudes and wavelengths.

5.3. Preferential porphyroblast growth on one limb of a regional fold

The four folds described herein have been affected by strongly non-coaxial deformation with dominantly the one shear sense at least once during their history of development. This occurred during the formation of both sub-vertical and sub-horizontal foliations in terms of the history recorded by the porphyroblast inclusion trails. One dominant shear sense (clockwise looking north) accompanied all phases of porphyroblast growth in the Strathalbyn anticline (Fig. 10a). This also occurred during the development of FIA 3 for garnet and FIA 1 for staurolite in the Bolton syncline (Fig. 10b), FIA 4 and FIA 5 on the east limb of the Spring Hill synform (Fig. 10c) and FIA 2 for the Pomfret dome (Fig. 10d). In the past, development of spiral inclusion trail geometries was commonly attributed to rotation of the porphyroblast. However, the data presented in Fig. 10 indicate that

1. Both asymmetries are usually present as shown in Fig. 10b–d.
2. Opposite asymmetries can dominate for the same FIA set on opposite limbs of the fold as shown for FIA 4 in Fig. 10c for the Spring Hill synform.

This strongly supports models for the development of spiral-shaped inclusion trails during folding without rotation of the porphyroblasts, such as those described by Stallard and Hickey (2001a,b) and Bell and Chen (2002), without the development of major shear zones (cf., Williams and Jiang, 1999). This data also supports a strong role for microstructural control on sites for the nucleation and growth of porphyroblasts (e.g., Bell and Hayward, 1991), and this aspect will be developed further in subsequent papers as it has considerable significance for metamorphic geologists.

5.4. Multiple phases of garnet growth

The advent of internally consistent thermodynamic datasets has provided a greater understanding of the stability of mineral assemblages through P–T space (e.g., Holland and Powell, 1985, 1998; Berman, 1991). These datasets show that the stability of garnet expands when MnO is included in the traditional KFMASH model system (Spear and Cheney, 1989; Symmes and Ferry, 1992; Mahar et al., 1997; Tinkham et al., 2001). Furthermore, pseudosections constructed using these datasets for the MnKFMASH and MnNCKFMASH systems show that the stability of garnet for varying bulk compositions extends to much higher and lower pressures and temperatures than the univariant reactions in KFMASH petrogenetic grids (e.g., compare Spear and Cheney, 1989 with Mahar et al., 1997 and Tinkham et al., 2001); P–T pseudosections are phase diagrams specific to a fixed bulk composition that provide a map of stable mineral assemblages in P–T space for a particular rock. This supports the widespread presence and multiple growth of garnet in rocks ranging from greenschist to amphibolite facies for a wide range of bulk compositions. No one sample in the areas where FIAs were measured contained more than four FIAs, and more typically they contain one or two FIAs per sample. This implies that most commonly there were only one or two periods of garnet growth recorded in any one sample, although in some there are at least four (e.g., Bell and Welch, 2002). Where reactivation is active on a fold limb and inhibits growth, a porphyroblast—in reaction such as the initial growth of garnet, may be become significantly overstepped. If this occurs after a core has nucleated and stabilized, reactivation may reduce or prevent further growth until a favourable pattern of deformation partitioning recommences. Variation in the bulk composition of rocks in the study areas could account for multiple phases of porphyroblast growth through P–T space. However, it does not account for the frequency of growth on a particular fold limb, especially since samples were taken from the same lithologies folded from limb to limb in all of the study areas.

5.5. Significance of the individual foliations preserved in porphyroblasts

Once regional scale folds have formed, our data suggests that it is easier for the limbs of those folds to take up the effects of subsequent shortening by reactivation, than for a new foliation to form, except where the orientation of the limb is such that it cannot reactivate. Any new foliations that are created should begin to form against a porphyroblast rim before they develop in the matrix because the porphyroblast is a competent object that generally takes up no strain and the preservation of truncational

foliations in porphyroblast rims and their obliteration from the matrix supports this (e.g., Bell and Hayward, 1991). However, the data in Fig. 10 suggests that such newly developed foliations will potentially be obliterated by reactivation of the compositional layering in that fold limb in the next event or the one after that and so the main metamorphic schistosity tends to be that parallel to bedding. Each newly developed foliation may therefore only represent a relatively small amount of shortening and shear, and result in little modification of the larger regional fold as shown in Fig. 12.

6. Conclusions

(1) Apparent regional folding of a young matrix foliation is not always a good guide as to the timing of the regional antiform or synform in question. Such folds could have formed very early during the history of deformation. Younger foliations forming with sub-horizontal orientations transect most regional folds. They can be readily rotated by reactivation of the folded layering as they form, as well as by subsequent horizontally directed bulk shortening, such that they appear to pre-date the regional fold.

(2) Sigmoidal, staircase and spiral-shaped inclusion trails of various asymmetries commonly change in frequency across early-formed regional fold hinges, suggesting that they formed as a result of the interplay between subsequent cleavage development and the differently dipping fold limbs, rather than development within a shear zone and rotation across the fold.

(3) The amount of porphyroblast growth can change across early-formed regional fold hinges as a function of the shear sense operating during the development of a younger foliation. Increased porphyroblast nucleation and growth occurs where the shear sense operating on a developing foliation is antithetic to the fold limb, such that reactivation or shear along the fold limb cannot readily occur. This leads initially to more coaxial deformation of the remains of previously formed foliations lying at a high angle to the axial plane and, as a direct result, to more sites for nucleation and growth of porphyroblasts.

Acknowledgements

We acknowledge and thank Haakon Fossen, Rick Law, Cees Passchier, Paul Williams and Adolph Yonkee for reviews of early versions of the manuscript. We found their many suggestions for its improvement very helpful. We thank K. Schulmann and Mike Williams for their reviews of this version and their suggestions for its improvement were excellent. We acknowledge the ARC (Australian Research Council) for research support for our work in the Appalachians. The Departamento de Geodinamica at the Universidad de Granada provided facilities that allowed a major revision of the manuscript to be made.

References

Adshead-Bell, N.S., Bell, T.H., 1999. The progressive development of a macroscopic upright fold pair during five near-orthogonal foliation-producing events: complex microstructures versus a simple macrostructure. Tectonophysics 306, 121–147.

Aerden, D.G.A.M., 1994. Kinematics of orogenic collapse in the Variscan Pyrenees deduced from microstructures in porphyroblastic rocks from the Lys-Caillaouas Massif. Tectonophysics 236, 139–160.

Aerden, D.G.A.M., 1996. The pyrite-type strain fringes from Lourdes, France: indicators of Alpine thrust kinematics in the Pyrenees. Journal of Structural Geology 18, 75–92.

Aerden, D.G.A.M., 1998. Tectonic evolution of the Montagne Noire and a possible orogenic model for syn-collisional exhumation of deep rocks, Hercynian belt, France. Tectonics 17, 62–87.

Bell, T.H., 1981. Foliation development: the contribution, geometry and significance of progressive bulk inhomogeneous shortening. Tectonophysics 75, 273–296.

Bell, T.H., 1986. Foliation development and refraction in metamorphic rocks: reactivation of earlier foliations and decrenulation due to shifting patterns of deformation partitioning. Journal of Metamorphic Geology 4, 421–444.

Bell, T.H., Chen, A., 2002. The development of spiral-shaped inclusion trails during multiple metamorphism and folding. Journal of Metamorphic Geology 20, 397–412.

Bell, T.H., Hayward, N., 1991. Episodic metamorphic reactions during orogenesis: the control of deformation partitioning on reaction sites and duration. Journal of Metamorphic Geology 9, 619–640.

Bell, T.H., Hickey, K.A., 1997. Distribution of pre-folding linear movement indicators around the Spring Hill Synform, Vermont: significance for mechanism of folding in this portion of the Appalachians. Tectonophysics 274, 275–294.

Bell, T.H., Hickey, K.A., 1998. Multiple deformations with successive sub-vertical and sub-horizontal axial planes: their impact on geometric development and significance for mineralization and exploration in the Mount Isa region. Economic Geology 93, 1369–1389.

Bell, T.H., Johnson, S.E., 1989. Porphyroblast inclusion trails: the key to orogenesis. Journal of Metamorphic Geology 7, 279–310.

Bell, T.H., Johnson, S.E., 1992. Shear sense: a new approach that resolves problems between criteria in metamorphic rocks. Journal of Metamorphic Geology 10, 99–124.

Bell, T.H., Welch, P.W., 2002. Prolonged Acadian orogenesis: revelations from foliation intersection axis (FIA) controlled monazite dating of foliations in porphyroblasts and matrix. American Journal of Science 302, 549–581.

Bell, T.H., Fleming, P.D., Rubenach, M.J., 1986. Porphyroblast nucleation, growth and dissolution in regional metamorphic rocks as a function of deformation partitioning during foliation development. Journal of Metamorphic Geology 4, 37–67.

Bell, T.H., Hickey, K.A., Wang, J., 1997. Spiral and staircase inclusion trail axes within garnet and staurolite porphyroblasts from the Bolton Syncline, Connecticut: timing of growth and the effects of fold development. Journal of Metamorphic Geology 15, 467–478.

Bell, T.H., Hickey, K.A., Upton, G.J.G., 1998. Distinguishing and correlating multiple phases of metamorphism across a multiply deformed region using the axes of spiral, staircase and sigmoidally curved inclusion trails in garnet. Journal of Metamorphic Geology 16, 767–794.

Berman, R.G., 1991. Thermobarometry using multi-equilibrium calculations: a new technique with petrological application. Canadian Mineralogist 29, 833–855.

Busa, M.D., Gray, N.H., 1992. Rotated staurolite porphyroblasts in the Littleton Schist at Bolton, Connecticut, USA. Journal of Metamorphic Geology 10, 627–636.

Davis, B.K., 1993. Mechanism of emplacement of Cannibal Creek Granite with special reference to timing and deformation history of the Aureole. Tectonophysics 224, 337–362.

Elliot, D., 1976. The energy balance and development mechanisms of thrust sheets. Philosophical Transactions of the Royal Society of London A283, 289–312.

Ham, A.P., 2001. Integration of porphyroblast growth with the microstructural and thermal histories during fold development, in the Acadian orogeny of the Vermont Appalachians. Unpublished PhD Thesis, James Cook University, Townsville, Australia. 330 pp.

Hayward, N., 1992. Microstructural analysis of the classic snowball garnets of southeast Vermont. Evidence for non-rotation. Journal of Metamorphic Geology 10, 567–587.

Hickey, K., Bell, T.H., 1999. Behaviour of rigid objects during deformation and metamorphism. A test using schists from the Bolton Synform, Connecticut. Journal of Metamorphic Geology 17, 211–228.

Hickey, K.A., Bell, T.H., 2001. Timing macroscopic folds in multiply deformed terrains. Bulletin of the Geological Society of America 113, 1282–1298.

Hobbs, B.E., Means, W.D., Williams, P.F., 1976. An Outline of Structural Geology. McGraw-Hill, NY. 571 pp.

Holland, T.J.B., Powell, R., 1985. An internally consistent thermodynamic dataset with uncertainties and correlations: 2. Data and results. Journal of Metamorphic Geology 3, 343–370.

Holland, T.J.B., Powell, R., 1998. An internally consistent thermodynamic data set for phases of petrological interest. Journal of Metamorphic Geology 16, 309–343.

Johnson, S.E., 1990. Deformation history of the Otago Schists, New Zealand from progressively developed porphyroblast/matrix microstructures: cyclic uplift-collapse orogenesis and its implications. Journal of Structural Geology 12, 727–746.

Jones, K.A., 1994. Progressive metamorphism in a crustal-scale shear zone: an example from the Leon region, north-west Brittany, France. Journal of Metamorphic Geology 12, 69–88.

Jones, C.H., Unruh, J.R., Sonder, L.J., 1996. The role of gravitational potential energy in active deformation in the southwestern United States. Nature 381, 37–41.

Lyons, J.B., 1955. Geology of the Hanover Quadrangle, New Hampshire–Vermont. Bulletin of the Geological Society of America 66, 106–146.

Mahar, E.M., Baker, J.M., Powell, R., Holland, T.J.B., 1997. The effect of Mn on mineral stability in metapelites. Journal of Metamorphic Geology 15, 223–238.

Offler, R., Fleming, P.D., 1968. A synthesis of folding and metamorphism in the Mt. Lofty Ranges, South Australia. Journal of the Geological Society of Australia 15, 245–266.

Ratcliffe, N.M., Armstrong, T.R., 1996. Digital bedrock geologic map of the Saxtons River 7.5% × 15% Quadrangle, Windham and Windsor Counties, Vermont. U.S. Geological Survey Open-File Report 96-52-A.

Ratcliffe, N.M., Armstrong, T.R., Aleinikoff, J.N., 1997. Stratigraphy, geochronology, and tectonic evolution of the basement and cover rocks of the Chester and Athens Domes. In: Grover, T.W., Mango, H.N., Hasenohr, E.J. (Eds.), Guidebook for Field Trips in Vermont and Adjacent New Hampshire and New York. 89th Annual Meeting of the New England Intercollegiate Geological Conference, Rutland, Vermont B6, pp. 1–55.

Rey, P., Vanderhaeghe, O., Teyssier, C., 2001. Gravitational collapse of continental crust: definitions, regimes, mechanisms and modes. Tectonophysics 342, 435–449.

Robinson, P., Tucker, R.D., 1982. Discussion of the Merrimack synclinorium in northeastern Connecticut by John Rodgers. American Journal of Science 282, 1735–1743.

Royden, L., 1996. Coupling and decoupling of crust and mantle in convergent orogens: implications for strain partitioning in the crust. Journal of Geophysical Research 101, 17679–17705.

Spear, F.S., Cheney, J.T., 1989. A petrogenetic grid for pelitic schists in the system SiO_2–Al_2O_2–FeO–MgO–K_2O–H_2O. Contributions to Mineralogy and Petrology 101, 149–164.

Stallard, A.P., Hickey, K.A., 2001a. Fold mechanisms in the Canton Schist: constraints on the combination of flexural flow. Journal of Structural Geology 23, 1865–1881.

Stallard, A.P., Hickey, K.A., 2001b. Shear zone vs. folding origin for spiral inclusions in the Canton Schist. Journal of Structural Geology 23, 1845–1864.

Symmes, G.H., Ferry, J.H., 1992. The effect of whole rock MnO content on the stability of garnet in pelitic schist during metamorphism. Journal of Metamorphic Geology 10, 221–237.

Tinkham, D.K., Zuluaga, C.A., Stowell, H.H., 2001. Metapelite phase equilibria modelling in MnNCKFMASH: the effects of variable Al_2O_3 and MgO/(MgO + FeO) on mineral stability. Geological Materials Research 3 (1), 1–41.

Williams, P.F., Jiang, D., 1999. Rotating garnets. Journal of Metamorphic Geology 17, 367–378.